ELSEVIER

Coordination Chemistry Reviews 226 (2002) 17–38

COORDINATION CHEMISTRY REVIEWS

www.elsevier.com/locate/ccr

Toward understanding nephelauxetism: interelectronic repulsion in gaseous d^q ions computed by Kohn–Sham DFT☆

Christian Anthon, Claus E. Schäffer *

Department of Chemistry, Chemical Laboratory I, University of Copenhagen, H.C. Ørsted Institute, Universitetsparken 5, DK-2100 Copenhagen 5, Denmark

Received 11 April 2001; accepted 15 October 2001

Contents

Abstract

The nephelauxetic phenomenon is reviewed. So is the newest formulation of the Slater–Condon–Shortley model (SCS) for the multiplet term energies of atomic d^q ions. This model is expressed as a sum of products of empirical parameters and their associated coefficient operators. The orthogonal-operators formalism is used by choosing Jørgensen's spin-pairing energy parameter D as one of the repulsion parameters when the other parameter required by the SCS model is the Racah parameter B. By restricting the coefficient operators further so as to make them orthonormal, B changes into the new parameter $E = (21/4)B$. D accounts for the energy separation of eigenstates with different spin and/or seniority, E for the final separation into the spatially different eigenstates. The numerical values of D and E exhibit directly the relative contributions of D and E to the average

Abbreviations: DFT, density functional theory; KS, Kohn–Sham; SCS, Slater–Condon–Shortley; ADF, Amsterdam density functional (package); LFT, ligand-field theory; AOM, angular overlap model; SSS, sum square splitting; RMS, root mean square (splitting); PW91, Perdew–Wang 91 (functional); GC, gradient corrected (functional); LDA, local density approximation; AOC, average of configuration; SCF, self consistent field.

☆ Presented at the 50th anniversary symposium of the Coordination Chemistry Section of the Japanese Chemical Society September 2000.

* Corresponding author. Tel.: +45-35320121; fax: +45-35320133.

E-mail addresses: anthon@kiku.dk (C. Anthon), ces@kiku.dk (C.E. Schäffer).

PII: S0010-8545(01)00449-0

configurational splitting. The parameter set $\{D, E\}$ is equivalent to the SCS set $\{F^2, F^4\}$ as well as to the Racah set $\{C, B\}$ even though these sets are not associated with orthogonal operators so that cross products, as for instance CB, enter the expressions for the average configurational splitting. Moreover, neither conventional parameter set provides a visualizable interpretation of the energetic functioning of its parameters upon the eigenstate energy separations. The symmetry problem of the two-electron part of Kohn–Sham DFT is discussed in the framework of the SCS model. With the future perspective of mimicking ligand-field theory and, in particular, of dealing with the full nephelauxetic phenomenon non-empirically, the atomic part of the phenomenon is handled by calculation of the parameters D and E successfully for numerous gaseous ions with $3d^q$ configurations. The Amsterdam Density Functional package (ADF) has been used in a two-step procedure. First, all the Kohn–Sham self-consistent field d-orbitals of the $3d^q$ configurations as well as all the inner core orbitals were determined using population numbers of $q/10$ for all the 3d-spin–orbitals, that is, by doing the average-of-configuration calculation. Secondly, all these orbitals were frozen in all the subsequent calculations on the same system. Here density distributions of α and β electrons were defined by integer occupation numbers of d-spin–orbitals corresponding to single Slater determinants. On grounds of principle, complex orbitals were found not to be usable. The ADF energy associated with a real determinant was—apart from an additive constant—taken to correspond to the expectation value of the interelectronic repulsion operator acting on the d^q part of this determinant. A characteristic property of the method is that the energy is expressed by a sum over contributions from the Coulomb and the exchange-correlation functional. It has turned out that for real d-orbitals both of these terms independently obey the symmetry restrictions as well as the special SCS restrictions of the d^q assumption. However, the two functionals are not commensurable. They give different parametric results. Nevertheless, by averaging the total energy results from using a gradient-corrected (GC) set of functionals over the configuration d^q, values for the SCS parameters that are better than those of Hartree–Fock calculations are obtained. In the local density approximation (LDA) the exchange-correlation functionals were found to provide the same energy for all real Slater determinants with the same value for M_S, which means that the exchange-correlation part of the energy corresponds to $B = E = 0$. However, the Coulomb functional invariably exaggerates the values of the E parameter so that LDA functionals end up giving fairly reasonable values of E, as well as D. We have obtained a complete bridge between KS-DFT in the form of ADF and the atomic part of ligand-field theory.

Keywords: Density functional theory, Nephelauxetic phenomenon, Interelectronic repulsion, Excited states, Ligand-field theory, Real orbitals

1. Introduction

This review is about a Density Functional Study of the Slater–Condon–Shortley (SCS) part of ligand-field theory on $3d^q$ systems.

Ligand-field theory is a semi-empirical model theory embodying a one-electron part, the ligand field (and spin–orbit coupling), and an electron-pair part, the interelectronic repulsion between all the pairs of electrons within the d^q configuration. The model is semi-empirical and parametrical in the sense that its energy expressions are linear combinations of energy parameters whose coefficients are purely theoretical and whose numerical values are determined by comparison with experimental results.

All the empirical parameters vary regularly with the central ions as well as with their chemical environments and their absolute and relative numerical values have served to rationalize a great deal of the chemistry of classical complexes. This is the reason for the popularity of ligand-field theory as well as for its perseverance in the text book literature. However, over the last 50 years it has been a problem that the values of the empirical parameters could not be reproduced by computational chemistry.

Density functional theory (DFT) has recently had a steadily increasing ubiquity in the chemical literature [1]. This is primarily due to this theory's ability to lend itself to handling large chemical systems with much less effort than other methods that give results of comparable quality. Another reason is that the results of KS-DFT seems to be more transparent for the chemist than do the results of the so-called ab initio methods.

Kohn–Sham-Density functional theory (KS-DFT) is a possible supplementary tool for the experimentalist, which may become of equal importance to the various spectroscopic techniques and, in particular, to results of X-ray diffraction experiments since it is perhaps foremost in predicting structures that KS-DFT has shown its remarkable ability [2].

Some of the main problems of KS-DFT exhibit themselves when it comes to handling degenerate ground and excited states within the same classifying configuration as the ground state. One speaks about the symmetry dilemma of KS-DFT. For a solution to this problem and discussions at a much more sophisticated level than that of the present paper, see Ref. [3], and for specific discussion of atomic multiplets, see [4]. The present paper is a different kind of contribution to the elucidation of these problems. Our starting point as far as DFT is concerned is the Amsterdam density functional package [5,6] (ADF) which is now quite acknowledged. ADF utilizes Kohn–Sham DFT [7] (KS-DFT) where the essence derives from the occupation numbers of spin–orbitals. Our paper assumes this framework.

We are interested in mimicking ligand-field theory by using KS-DFT. Ligand-field theory is fundamentally a one-electron theory whose empirical parameters represent the perturbation of the d-orbitals by the chemical

environment of the central ion. However, when it is to be used to describe systems with more than one electron, LFT has traditionally been combined with the purely atomic theory called the Slater–Condon–Shortley (SCS) theory of interelectronic repulsion. It turns out that even though we are concerned with an atomic theory, a considerable reduction of the interelectronic repulsion parameters of the corresponding gaseous ions is observed, a result that can be interpreted as an expansion of the radial functions of the d-orbitals, or in other words, an expansion of the electronic density distribution of the d-electrons. This general phenomenon was named the nephelauxetic phenomenon. We are particularly interested in trying to elucidate this by KS-DFT. However, in the present review we limit ourselves to the atomic case and show that it is possible to calculate the interelectronic repulsion parameters by ADF–DFT.

2. Ligand-field theory: the parametrical d^q model

2.1. The history: physical and semi-empirical viewpoints

Our particular interest is in ligand-field theory (LFT), which revolutionized inorganic chemistry 50 years ago [8] and allowed an understanding of what is today called d–d spectra or ligand-field spectra of metal complexes. In the early 30s it had been invented as crystal-field theory by the physicists [9] who also realized its symmetry connection with molecular orbital theory [10,11]. Then around 1950 it was noticed by chemists [12–19] and it soon advanced into the forefront of chemistry but it only stayed there for about a decennium. Then the interest leveled off and already when the angular overlap model (AOM) was new, the subtitle of a paper in 1965 was: 'An attempt to revive the ligand-field theories' [20]. In fact, the AOM did so, but only in the sense that the further development of the subject never died out. Today the situation is that the treatment of transition metal chemistry in text books is quite dependent on LFT, and every chemist knows well what LFT is and is able to apply it qualitatively, but few chemists know much more than that even though quantification was always an essential feature of LFT.

In the early days of ligand-field theory in chemistry, crystal-field theory was the term used and the whole construction was considered to be a physical model where the effect of the ligands was an electrostatic one and only the perturbation of the d-electrons was in focus. This physical model allowed—at least in principle—Δ as well as the SCS parameters F^2 and F^4 (see Section 3.1) to be calculated on the basis of the radial functions associated with the d-orbitals, which were those of the corresponding gaseous ion.

However, the chemists soon realized that this physical model was unrealistic and the name and the conceptual use of the model were changed. The term: ligand field was coined, but mathematically the crystal-field model and the ligand-field model are equivalent.

This history of the change of name from crystal-field to ligand-field theory is fuzzy. Actually, the change of name took place for two partially independent reasons. The first reason was that a model which originally was a solid state model was now used for individual complex ions containing ligands. The second reason was that in the hands of chemists, the semi-classical electrostatic model was quickly discarded as a physical model. Let us just recall one point: H_2O and OH^- have almost the same Δ values. But clearly, in an electrostatic model, the ion with the negative charge would have been expected to be the stronger perturber. There were many other reasons for discarding the electrostatic interpretation of the empirical parameters [21], but the power of the model in organizing and rationalizing spectroscopic and magnetic results did not depend on this interpretation. Ligand-field theory was therefore used as the name for the semi-empirical version of the model that consisted of empirical parameters whose coefficients were theoretical, i.e. were calculated by integrations over the angular functions of the d-orbitals or determined by symmetry. This view of the model as a semi-empirical rather than a physical model also applied to the two-electron part of ligand-field theory. This part was most of the time expressed in terms of the Slater–Condon–Shortley model, which also for atoms had been used semi-empirically. Ferguson, however—in an attempt to view nephelauxetism in an alternative way—used the SCS model, parametrically extended with the Trees' parameter, as an alternative version of the SCS model that could be simultaneously used as a semi-empirical (as regards the Trees' parameter) and a physical model [22] (regarding the SCS parameters F^2 and F^4, see also Section 2.3).

Consistent qualitative molecular orbital explanations for the chemical variations of the empirical parameters soon became accepted by practically the whole chemical community. Gerloch and Woolley later made an exception here, which is hard to communicate to a chemical readership [23,24]. Three facts are, however, easy to state: first, their cellular-ligand-field is mathematically not only equivalent but identical to the angular overlap model. Secondly, their practical parametrical connection of the cellular model with experiments is also identical with that used with the angular overlap model in that they realize that only energy differences are observables [25–27]. Thirdly, their interpretation of the parameters is nevertheless different from that associated with the conventional molecular-orbital-oriented angular overlap model. It is our expectation that KS-DFT may help clarifying these differences of opinion.

2.2. Observed oxidation states and nephelauxetism

LFT is a combination of the ligand-field and the Slater–Condon–Shortley (SCS) theory of interelectronic repulsion [28,29]. Both the one-electron and the SCS theory are parametrical, which means that they are used to transform data (spectroscopic and magnetic) into empirical parameters. The quantitative strength of these combined theories, which we like to call the parametrical d^q model [30–32], is that apparently unrelated data may be transformed into parameters that are directly comparable, and once these parameters have been obtained, remarkable regularities are found, e.g. the spectrochemical and nephelauxetic series of ligands and of central ions [33].

LFT obtained many qualitative results that are so certain that they can be used to test the best theories in this computer age. For example, there are no exceptions to the rule that

$$\Delta \equiv h(e_g) - h(t_{2g}) > 0 \quad (1)$$

in octahedral complexes with a partially filled outer electron shell. h here refers to ligand-field one-electron energies and e_g and t_{2g} refer to the orbitals with predominantly d character, i.e. the orbitals carrying the electrons of this partially filled shell. The series of ligands with increasing Δ values associated with a given metal ion is almost independent of which metal ion. This series was identified as the spectrochemical series, which had been established in the past on the basis of pure empiricism. Cobalt(III) complexes, mainly of lower symmetry than octahedral and containing ligands or more than one kind, had been the experimental basis.

The inequality in Eq. (1) has some fundamental consequences: it allows a correct prediction of the symmetries of the ground state and the lower excited states of octahedral complexes to which any theory must comply.

The nephelauxetic phenomenon is the phenomenon that the experimentally determined interelectronic repulsion parameters are invariably diminished in complexes relative to the corresponding gaseous ions. This statement may give the impression of containing little more than a definition of the adjective nephelauxetic, but the phenomenon implies much more than that.

Let us begin by focusing upon the gaseous d^q ions. Gaseous d^q ions are examples of systems for which the oxidation number and the oxidation state are by their definitions equal and both equal to the charge of the ion. So we are on solid ground with atomic systems. Let us then observe the fact that the empirical interelectronic repulsion parameters for gaseous d^q ions, with fixed q, invariably decrease when the charge is decreased. For example, the empirically determined values of the Racah parameter B for the d^3 ions Cr^{3+} and V^{2+} are 0.093 and 0.076 μm^{-1}, respectively [29]. Returning to the concept nephelauxetic, i.e. cloud expanding, we then observe that when real chemistry enters the scene, complexation invariably leads to an effect on the repulsion parameters that mimics a reduction in charge, which is often considerable. For example, while the Racah parameter B has the value 0.093 μm^{-1} for the gaseous Cr^{3+} ion, the value for $Cr(CN)_6^{3-}$ is 0.053 μm^{-1} [34]. In other words, the central ion to ligand bond formation conserves q, but yet gives an apparent decrease of the charge on the central ion. For the typical ligand-field systems, q is an empirically determined integer, derivable from ligand-field spectra and magnetism. Then the oxidation state z of the ion in the complex is equal to the charge of the corresponding gaseous ion and the interrelationship between integers

$$z = g - q \quad (2)$$

is valid, when g is the IUPAC group number, e.g. 10 for Nickel, so that both q and z are known from ligand-field empiricism [32,35,36]. This empirically determined oxidation state is equal to the conventional oxidation number used in classifying the chemistries of metal complexes. Thus, complexation is accompanied by an invariant number of d-electrons, and an invariant oxidation state z, equal to the usual oxidation number, but associated with an apparent decrease of charge on the central ion. This non-integer decrease of charge is explained consistently by electronic charge from the ligands invading the central ion domain through the covalency involving central ion s- and p-orbitals. Thereby, the d-electrons are screened so that their cloud is expanded. In connection with this explanation, Jørgensen introduced the concept: central field covalency [33].

In conclusion, it is possible to talk about a typical ligand-field spectrum of, for example, a d^3 ion whereby, through Eq. (2), both q and z become empirically determined. In other words, the oxidation state z is equal to the formal oxidation number, just as it was the case by definition for the gaseous central d^q ion, but here the result is semi-empirical and based upon an observed ground-state, for instance for $q = 3$, $^4A_{2g}(O_h)$ combined with excited states $^4T_{2g}(O_h)$ and $^4T_{1g}(O_h)$ corresponding to the first and second spin-allowed absorption bands. All the states mentioned as well as their relative energies are typical of d^3 systems in octahedral environments. Thus $q = 3$ so that $z = 3$ for Cr^{3+} because $g = 6$ and $z = 2$ for V^{2+} because $g = 5$, in both cases according to Eq. (2). This equation which is true by definition for gaseous d^q systems practically never applies to gaseous atoms and singly positively charged ions because of s-electrons being contained in the configurations of their ground-states, but it practically always applies to metal complexes when $1 \leq q \leq 9$, and this is probably because the s-orbitals are now embod-

ied in antibonding molecular orbitals with an energy high enough to keep them empty [36].

2.3. Elaboration of the nephelauxetic phenomenon. Chemical regularities

The nephelauxetic phenomenon is the fact that repulsion parameters are invariably smaller in complexes than in the corresponding gaseous ions. Quantification of the phenomenon gives rise to very regular behavior with respect to variations of ligands as well as of central ions, which both provide nephelauxetic series [33,36–38] that are largely independent of the central ion and the ligand, respectively. Increasing nephelauxetism corresponds roughly to increasing covalency of the ligand-to-metal bond. Thus, F^- is the least nephelauxetic ligand and Br^- and CN^- the most nephelauxetic ones. The position of I^- in the nephelauxetic series of ligands is still unknown. Moreover, in the nephelauxetic series of central ions, the trend is that the more oxidizing ion experiences the larger nephelauxetic effect. If oxidizing also means particular propensity for ligand to metal charge transfer, the explanation of the nephelauxetic phenomenon becomes chemically consistent.

Another convincing fact about nephelauxetism is the following. Whereas, the chemical variation of the repulsion parameters in d^5 systems can be observed directly as the variation of the $^6S \rightarrow {}^4G$ transition energy, where this atomic ion transition energy is found directly as a ligand-field transition energy of octahedral and tetrahedral complexes, the parameters for most other d^q configurations are deeply buried in the ligand-field spectra so that the parametrical d^q model has to be applied quantitatively. Mathematically completely different data transformations are then required depending on the configuration in question, and it is necessary to go beyond the Hartree–Fock level (within the d^q configuration limitation of the ligand-field model) in that sub-configuration interaction is essential. A d^6 example will illustrate this with the spectra of octahedral low-spin cobalt(III) complexes, which exhibit two spin-allowed absorption bands $^1A_{1g} \rightarrow {}^1T_{1g}(O_h)$ and $^1A_{1g} \rightarrow {}^1T_{2g}(O_h)$. In the approximation of pure cubic sub-configurations the first band lies at $\Delta - C$ and the second band at $\Delta - C + 16B$ where C and B are the Racah repulsion parameters [39] and Δ is the energy difference between the $e_g(O_h)$ and the $t_{2g}(O_h)$ orbitals (Eq. (1)). In this approximation the Racah parameter B could have been obtained from the energy difference between the two excited states. However, this approximation, which ignores the sub-configuration interaction between five $^1A_{1g}$ terms, four $^1T_{1g}$ terms and seven $^1T_{2g}$ terms, is not useful in establishing the nephelauxetic series. For this purpose the 5×5 matrix of $^1A_{1g}$, the 4×4 matrix of $^1T_{1g}$ and the 7×7 matrix of $^1T_{2g}$, which are non-diagonal in the repulsion parameters, have to be diagonalized, thus taking the sub-configuration interaction into account [39]. The important point is that a most involved—but completely well-defined—data transformation is required in order to obtain the regularities derivable from the experimental absorption spectra. In other words, LFT, quantitatively applied, has a remarkable ability to bring order into chaos and a remarkable internal consistency. These diagonalizations had already been properly done as a basis for the nephelauxetic data provided by Jørgensen and Griffith in the early 60s [33,39].

The primary outcome of the fitting of the spectra is—in addition to the one-electron information about the ligand-field itself—the magnitudes of the two-electron parameters applicable to the complex in question. These values then have to be compared with the magnitudes of the same parameters applicable to the corresponding gaseous ion where one has to note that the word 'corresponding' here implies that the oxidation state of the central ion is determined on the basis of its ligand-field spectra according to Eq. (2).

In practice, the spectral information did not always allow two repulsion parameters to be determined. Therefore, with the exception of Ferguson [22] who argued that the two independent repulsion parameters for physical reasons had inherently different radial dependencies (Section 2.1), the ratio between the repulsion parameters found for the gaseous system was assumed to be transferable to the complex.

As a quantification of the nephelauxetic phenomenon, the nephelauxetic ratio β was used, where

$$\beta = \frac{B_{\text{complex}}}{B_{\text{gaseous ion}}} \tag{3}$$

β was often assumed to be independent of which repulsion parameter was used. Anyway, the same nephelauxetic series of ligands was observed from the d^5 transition energy referred to above, i.e.

$$\beta = \frac{[H(^4G) - H(^6S)]_{\text{complex}}}{[H(^4G) - H(^6S)]_{\text{gaseous ion}}} = \frac{[2B + C]_{\text{complex}}}{[2B + C]_{\text{gaseous ion}}} \tag{4}$$

where ^4G can be observed as the lower-energy $^4E_g(O_h)$ excited state in spin-forbidden intra sub-configuration $t_{2g}^3 e_g^2 \rightarrow t_{2g}^3 e_g^2$ transitions in octahedral and tetrahedral high-spin d^5 complexes.

However, the main body of the empirical basis for the nephelauxetic series of ligands came from the spectra of Ni(II) and Cr(III) complexes where the spectral information employed came from the spin-allowed transitions only, and where the Racah parameter B therefore was the one determined, and Eq. (3) the expression used. The low-spin Co(III) complexes also contributed considerably and here the Racah parameter C was only moderately involved in the nephelauxetic ratios and not at all in the ordering of the ligands in the nephelauxetic series.

It was suggested that there were at least two contributions to the covalency which were to explain the nephelauxetic phenomenon. In Jørgensen's paper, they were named the central-field covalency, a spherical term, and the symmetry-restricted covalency, an octahedral term [33].

The central-field covalency was explained as a screening effect on the d-electrons arising from electronic charge from the ligands transgressing the volume of the d-electrons, thus partially screening them from their central ion nucleus [36]. This screening effect should be caused by covalency involving the empty s- and p-orbitals of the central ion and—for an octahedral complex—this is a pure ligand-field effect whose only effect upon the d-electrons is a decrease of their repulsion parameters due to an expansion of the d-orbitals and an associated increase in their average distances (or, more specifically, decrease of their average reciprocal distances and therefore decrease of their repulsion parameters).

The symmetry-restricted covalency is one involving the d-orbitals more explicitly and this brings us away from simple ligand-field theory, i.e. the parametrical d^q model, and over into some molecular orbital model. The symmetry-restricted covalency was never quantified but it was considered nevertheless to be observable by the fact that if the ratio between the two repulsion parameters was assumed to be constant on going from the gaseous ion to the complex (Eq. (4)), then the intra t_2^3 sub-configuration transitions of Cr(III) complexes, the ruby lines so-called, were invariably blue-shifted compared with their expected positions on the basis of the B (and thereby also C) values, known from the spin-allowed transitions.

In spite of the fact that expansion of the d-orbitals might well diminish F^2 and F^4—and thereby B and C (Section 3.1) to a different extent [22], it was usually assumed that the ratio between the repulsion parameters did not alter much on complexation. Anyway, it was assumed that the chemical effects on the nephelauxetic ratio β was so dominating that the difference between $\beta(F^2)$ and $\beta(F^4)$ would be insignificant. Therefore, the ruby-line phenomenon was explained beyond the ligand-field model by assuming the nephelauxetic influence upon the π-interacting t_{2g} electrons to be smaller than that on the σ-interacting e_g electrons. The ruby line phenomenon was named 'symmetry-restricted covalency' [33], but this explanation was never developed into a quantitative model. This problem of whether or not one nephelauxetic parameter suffices is still an open one that might be elucidated by KS-DFT.

In a previous paper [32] we estimated that the two-electron operator contribution to the sum-square-splitting (SSS) in the d^7 system $[CoI_4]^{2-}$ made up 95% and the tetrahedral ligand-field only 5% (Section 3.1). This example, even if rather extreme, shows the quantitative importance of the interelectronic repulsion. Moreover, the total SSS in $[CoI_4]^{2-}$ is, in spite of the ligand-field contribution contained in it, considerably smaller than in the gaseous Co^{2+} ion. This is of course another consequence of nephelauxetism.

2.4. Status and future of ligand-field theory

The parametrical d^q model may be viewed as a machinery which under suitable conditions allows us to perform a data reduction where spectroscopic and magnetic data from chemical systems of d^q type are transformed into numerical values for a limited number of empirical parameters. Such data reductions have been performed in the past, and because the parameters themselves have been comparable and of course their numerical values also comparable, an orderly quantitative overview of d^q systems has resulted. However, most of the easy experiments have been done and new or at least improved experimental techniques are necessary to get much further. Most of the successes have been associated with high-symmetry systems. But even though the angular overlap model of the ligand field embraces low-symmetry systems as well, the successes here have been counteracted by nature itself. The problem is overparametrization. When symmetry is decreased, the number of parameters required invariably increases, but only in rare cases does the number of observations increase correspondingly. Therefore, we are close to the limit where the known chemical systems no longer provide enough information for feeding the ligand-field machinery. Under these circumstances, new strategies are necessary if one wants to keep the huge ligand-field data bank still eye-catching.

It is our special hope to be able to use KS-DFT for elucidating and quantifying the nephelauxetic phenomenon. This is, however, the future perspective of our present paper which is only about atomic ions. In more general terms, we see KS-DFT as the first possible theory which is at least in principle non-empirical and which can be used as a supplement to LFT, and we shall apply KS-DFT in this spirit. This means that we shall be interested only in energy differences and our primary purpose is to mimic LFT altogether rather than utilizing KS-DFT optimally.

In the world of the professional quantum chemists there were also approaches to show that ligand-field theory could not be theoretically justified as a physical theory, and when it was generally acknowledged as a semi-empirical model 40 years ago, it was mostly held in contempt in the quantum circles. More recently, as computational chemistry gradually developed into becoming useful for the chemists, the quantum people realized that some of the qualitative results of the application of ligand-field theory were unavoidable and even its empirical parameters or at least their chemical variations could be interesting for the computational chemist. Perhaps the reason is that it is so difficult to extract insight out of the results of huge computations. Anyway, in recent years ligand-field theory seems more and more to go hand in hand with ab initio and

KS-DFT work in such a fashion that they fertilize each other, see, for example, [40,41].

However, it is unlikely that such a problem as over-parametrization will be solvable by computational support. It is more likely that we are at the practical limits of the parametrical d^q model, but a theoretical and computational elucidation of its estate is still highly desirable.

3. The parametrical d^q model and its Slater–Condon–Shortley (SCS) part

3.1. The orthonormal-operators formulation of the parametrical d^q model. Parametrization of SCS theory by the spin-pairing energy parameter D and its spatial complement E

Even though the ligand-field is a one-electron property, LFT must be extended to embody electron correlation when its domain is extended beyond one electron in the partially filled shell. Therefore, we call it the parametrical d^q model and write its barycentered Hamiltonian in the form

$$\hat{H} = \hat{H}_{\mathrm{V}} + \hat{H}_{\mathrm{R}} = \sum_i \hat{H}_{\mathrm{V}i} + \sum_j \hat{H}_{\mathrm{R}j} \tag{5}$$

where the hats symbolize operators and V and R represent the independently barycentered ligand-field and interelectronic repulsion terms and i and j their various parametrical components. Here, we restrict ourselves to systems of octahedral symmetry so that the ligand-field has only one component which is observable, the spectrochemical parameter Δ (Eq. (1)), whose part of the Hamiltonian we shall write as

$$\hat{H}_{\mathrm{V}} = \Delta\hat{\Delta} \tag{6}$$

where $\hat{\Delta}$ is a coefficient operator given by its matrix in a suitably chosen basis. Since the coefficients to Δ are invariably determined by symmetry, the operator $\hat{\Delta}$ is fully symmetry determined [42].

The reader who is unfamiliar with this formulation will appreciate the meaning of the definition of $\hat{\Delta}$ by the example of Eq. (7) where $\hat{\Delta}$ is given as a matrix of pure numbers in a well-known orbital basis

$$\begin{array}{c} \\ \mathrm{e}(z^2) \\ \mathrm{e}(x^2-y^2) \\ \mathrm{t}_2(yz) \\ \mathrm{t}_2(zx) \\ \mathrm{t}_2(xy) \end{array} \begin{array}{c} \begin{array}{ccccc} \mathrm{e}(z^2) & \mathrm{e}(\mathrm{x}^2-\mathrm{y}^2) & \mathrm{t}_2(\mathrm{yz}) & \mathrm{t}_2(\mathrm{zx}) & \mathrm{t}_2(\mathrm{xy}) \end{array} \\ \begin{bmatrix} 3/5 & 0 & 0 & 0 & 0 \\ 0 & 3/5 & 0 & 0 & 0 \\ 0 & 0 & -2/5 & 0 & 0 \\ 0 & 0 & 0 & -2/5 & 0 \\ 0 & 0 & 0 & 0 & -2/5 \end{bmatrix} \end{array} \tag{7}$$

When this matrix is multiplied by the parameter Δ, the energy matrix of the one-electron Hamiltonian of Eq. (6) is obtained.

There is nothing mysterious about the operator $\hat{\Delta}$ which is completely defined by Eq. (7). This matrix and its associated parameter might alternatively be written in condensed form as Eq. (8):

$$h(\mathrm{e_g}) = \tfrac{3}{5}\,\Delta \qquad h(\mathrm{t_{2g}}) = -\tfrac{2}{5}\,\Delta \tag{8}$$

in which the weights are implicitly contained in the symbols $\mathrm{e_g}$ and $\mathrm{t_{2g}}$.

The coefficient operator formalism, which associates every observable parameter with a corresponding operator, has several advantages as we shall see presently.

The important information of the matrix Eq. (7) could alternatively have been written with the first two diagonal elements replaced by unity and the last three by zero. This would have defined the same energy difference between the $\mathrm{e_g}(O_h)$ and the $\mathrm{t_{2g}}(O_h)$ electrons of the octahedral ligand-field. However, for all the applications of ligand-field theory, only energy differences are observables. Therefore, the barycentration illustrated in Eqs. (7) and (8) is a generally useful requirement to impose upon ligand-field considerations. We say that a barycentered operator is traceless, which means that any of its matrix representations has the sum of its diagonal elements equal to zero.

From the expression of Eq. (7), it is possible to set up the expression for $\hat{\Delta}$ in any d^q basis.

The repulsion terms of Eq. (5), parametrized in the Slater–Condon–Shortley model using Racah parameters, may be written as

$$\hat{H}_{\mathrm{R}} = C\hat{C} + B\hat{B} \quad \text{(barycentered)} \tag{9}$$

where the non-observable A term was made to disappear by barycentration of $\hat{H}_{\mathrm{R}}$ (Eq. (12)). In Eq. (9) the parametrical symbols with an added hat, as in Eq. (6), are symmetry-determined coefficient operators associated with their corresponding parameters. Here we shall use an alternative parametrization of $\hat{H}_{\mathrm{R}}$ embodying Jørgensen's spin-pairing energy parameter D [34] and its complementary one, denoted by E. E is for practical purposes the same parameter as the Racah parameter B, being given by the relation

$$E = \tfrac{21}{4}\,B \tag{10}$$

The reason for choosing E rather than B is that the numerical values of the positive parameters D and E are directly comparable because the lengths of their associated coefficient operators are equal. We shall return to this point presently.

The parameter D is given by

$$D = \tfrac{7}{6}\,(C + \tfrac{5}{2}\,B) \tag{11}$$

where the expression in parentheses is equal to the average value of the exchange integral between pairs of

real d-orbitals [34]. If one starts out from the Tanabe–Sugano energy matrices in terms of Racah parameters [39,43], one may transform these in our present parametrical set by introducing Eqs. (10) and (11), and, for barycentration,

$$A = \tfrac{14}{9}B - \tfrac{7}{9}C \tag{12}$$

The new parametrization then has the parametric repulsion Hamiltonian

$$\hat{H}_{\mathrm{R}} = D\hat{D} + E\hat{E} \quad \text{(barycentered)} \tag{13}$$

where the matrices of $\hat{D}$ and $\hat{E}$ for d^2 are diagonal (Eq. (14)) in a multiplet term basis.

$$H(^1S) = H_{\mathrm{av.}}(d^2) + \tfrac{112}{21}D$$
$$H(^1G) = H_{\mathrm{av.}}(d^2) + \tfrac{22}{21}D + \tfrac{10}{21}E$$
$$H(^3P) = H_{\mathrm{av.}}(d^2) - \tfrac{14}{21}D + 2E$$
$$H(^1D) = H_{\mathrm{av.}}(d^2) + \tfrac{22}{21}D - \tfrac{18}{21}E$$
$$H(^3F) = H_{\mathrm{av.}}(d^2) - \tfrac{14}{21}D - \tfrac{18}{21}E \tag{14}$$

Apart from the term $H_{\mathrm{av.}}(d^2)$, Eq. (14) is analogous to the condensed form of Eq. (7), given in Eq. (8). It represents 45 linear equations giving the parametrically expressed energies of the five multiplet terms, three singlets $S = 0$, $2S + 1 = 1$, $L = 0$, 2 and 4 (S, D, and G) and two triplets $S = 1$, $2S + 1 = 3$, $L = 1$ and 3 (P and F).

In Eq. (14) the average energy $H_{\mathrm{av.}}$ of the d^2 configuration, whose value depends on an external zero point, has been added so that we have

$$\hat{H}_{\mathrm{R}} = H_{\mathrm{av.}}\hat{H}_{\mathrm{av.}} + D\hat{D} + E\hat{E} \quad \text{(not barycentered)} \tag{15}$$

where the coefficient operator $\hat{H}_{\mathrm{av.}}$ is represented by the unit matrix independent of basis. If the first term of Eq. (15) is left out, a barycentered operator is obtained, when the weights of the multiplet terms are $(2S + 1)(2L + 1)$.The spin-pairing energy parameter D sees to it that the 30 triplet states embodied in ^3P and ^3F have the negative term $-\frac{2}{3}D$ in common (Hund's 1. rule) and the remaining parameter E gives a negative contribution to the energy of ^3F and a positive one to that of ^3P (Hund's 2. rule). By using the proper weights, it may be noted that $\hat{D}$ is barycentered on the whole configuration d^2 and $\hat{E}$ barycentered over the singlet and the triplet spaces separately and therefore also on their sum, i.e. d^2. The average contribution of $\hat{D}$ to the singlets is

$$\frac{112 + (9 + 5)22}{21(1 + 9 + 5)} = \frac{4}{3}D \tag{16}$$

and, as already mentioned, $-2/3D$ to the triplets so that

$$H_{\mathrm{av.}}(\text{singlets}) - H_{\mathrm{av.}}(\text{triplets}) = 2D \tag{17}$$

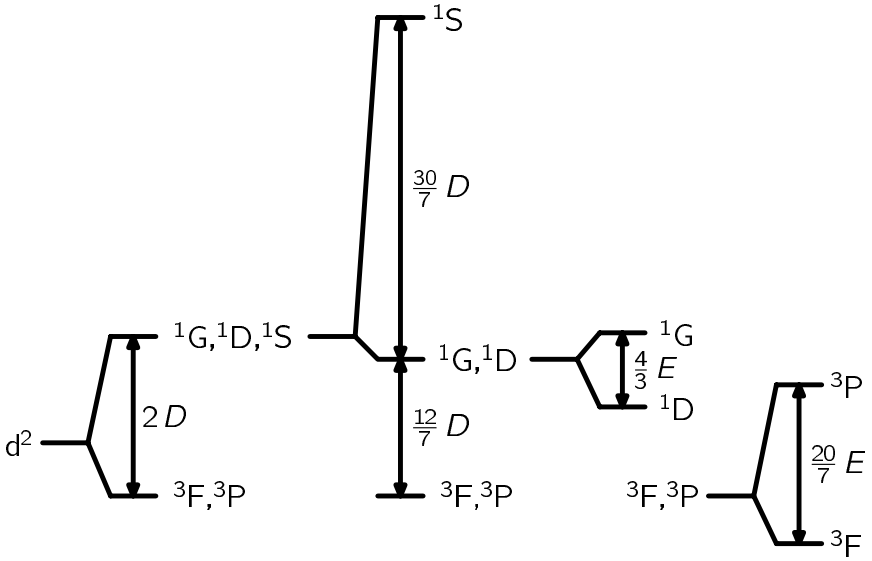

Fig. 1. Multiplet terms of d^2. Illustration of the barycentered operator $\hat{H} = D\hat{D} + E\hat{E}$. The horizontal line to the left represents the zero point of energy, $H_{\mathrm{av.}}(d^2) = 0$, d^2 referring to the 45 states of this configuration. It is instructive to think about $\hat{D}$ as acting in two consecutive steps from left to right. The first step then illustrates its inherent function as a separator for the total spin S. One might call this its function as a genuine spin-pairing energy operator where it acts on all the 45 states of d^2 with D as its genuine spin-pairing energy parameter. After this first step, the triplets are degenerate with energy $-(2/3)D$ and the singlets with energy $(4/3)D$ and the action of $\hat{D}$ exhausted within the triplet states. When using the concept of spin-pairing, one must keep in mind that the pairing of spins literary refers to M_S rather than S (see the discussion about spin flipping in subsection Section 3.3 and about M_S in the Appendix). In the second step in the figure, $\hat{D}$ separates ^1S with seniority, $v = 0$, from the other two singlets with seniority, $v = 2$, to provide the ^1D, ^1G pair with the energy change of $-(2/7)D$ and ^1S with the energy change of $(28/7)D$ conditioned by the barycenter rule. In other words, $\hat{D}$ is the total spin and seniority separator. $\hat{E}$ acts separately on the term pairs ^1D, ^1G and ^3P, ^3F and is therefore a double-functioned spatial separator (or an orbital separator, i.e. acting on the orbital part of the d^2 state functions, but not on orbitals).

Eq. (17) is an example of a general property of $\hat{D}$ as expressed in Eq. (18):

$$H_{\text{av.}}(S_0 - 1) - H_{\text{av.}}(S_0) = 2DS_0 \tag{18}$$

This expression, which is valid for all d^q, is formally analogous to the Landé interval rule. There is evidence that Eq. (18) has a validity far beyond the SCS model [44].

The meaning of the parameters D and E is further illustrated in Fig. 1, where the 45 states of d^2 have been placed at their barycenter (left), i.e. the average energy of the d^2 configuration is used as a zero point of energy. $\hat{D}$ has two functions: (1) it splits the spin states as we saw in Eq. (18); and (2) it separates ^1S from the other singlet terms ^1G and ^1D, which are left with the same energy contribution from $\hat{D}$.

If all the 1024 states of all d^q ($0 \le q \le 10$) configurations are considered together—and this is meaningful in the higher symmetry spheres—then we may say that we already have met a ^1S term, namely $^1S(d^0)$, and it turns out that this is what makes ^1S unique among the singlets. We say that $^1S(d^2)$ has seniority zero whereas all the other d^2 terms have seniority two. The example thus illustrates the general property of $\hat{D}$ that it also separates all the different seniorities of all d^q configurations. The operator $\hat{E}$ is spatial in character. It separates the multiplet terms of different spatial symmetry within each group of states having the same coefficient to D.

In order to illustrate the concept of orthogonal operators, it is useful to realize the analogy between Eqs. (8) and (14). This is easiest if Eq. (8) is rewritten as

$$h(e_g) = h_{\text{av.}}(d) + \tfrac{3}{5}\Delta \tag{19}$$
$$h(t_{2g}) = h_{\text{av.}}(d) - \tfrac{2}{5}\Delta$$

so that the matrix of $\hat{h}_{\text{av.}}$ is the unit matrix. If we consider the diagonals of $\hat{h}_{\text{av.}}(d)$ and $\hat{\Delta}$ as column vectors, then these vectors are orthogonal and we say that the two diagonal operators are orthogonal. So orthogonality of an operator on to $\hat{h}_{\text{av.}}$ is the same as the operator being barycentered. This particular orthogonality is especially useful for parametrizing l^q models because only energy differences are observables here.

Let us look a little closer at the concept of orthogonality of operators and the more restricted concept of orthonormal operators.

We shall do this by using as an example the operators of the configuration d^2, illustrated in Eq. (14) and in Table 2. We recapitulate a little more generally that a configuration d^q is a collection of $\binom{4l+2}{q}$ states whose energies can be described by two features. The first one is their average energy $H_{\text{av.}}(d^q)$, which depends on the choice of zero point. The second one is the energy splitting, which is the collection of state energies, measured relative to $H_{\text{av.}}(d^q)$, the barycentered energies so-called. They have the property that their sum equals zero. A measure of the average global splitting of the configuration d^q could then be chosen as the sum over the states of the absolute values of their barycentered energies. However, it turns out that the sum of the squares of these energies has especially useful properties. We have called this quantity, the sum-square-splitting, SSS. Since we distinguish between observed state energies and the corresponding energies calculated by some model theory, it is convenient to distinguish also between observed and calculated sum square splittings, SSS_{obs} and SSS_{calcd}, and if the SCS model is used, we obtain the equality $SSS_{\text{calcd}} = SSS_{\text{SCS}}$. We note that the observed and calculated value of $H_{\text{av.}}(d^q)$ is the same because our models are concerned with energy differences rather than absolute energies.

The sum-square-splitting SSS_{SCS} can be expressed in the form of a sum of contributions from the two splitting parameters D and E of our model. For this simple form to be valid, the associated coefficient operators must be orthogonal. Let us illustrate this by expressing SSS_{SCS} for d^2. By using Eq. (14) we obtain

$$\begin{aligned} SSS_{\text{SCS}} &= 1\left(\frac{112}{21}D\right)^2 + 9\left(\frac{22}{21}D + \frac{10}{21}E\right)^2 \\ &\quad + 5\left(\frac{22}{21}D - \frac{18}{21}E\right)^2 \\ &\quad + 9\left(-\frac{14}{21}D + 2E\right)^2 + 21\left(-\frac{14}{21}D - \frac{18}{21}E\right)^2 \\ &= \frac{400}{7}(D^2 + E^2) \end{aligned} \tag{20}$$

In an experiment where one has observed the energies of the five multiplet terms (and thereby their barycentered energies), SSS_{obs} would be calculated analogously. If the parametric values of D an E of Eq. (20) were found by a fitting procedure based upon the least squares method, this method would always see to it that SSS_{SCS} be smaller than SSS_{obs}, a kind of variation principle.

It is noteworthy that SSS_{SCS} of Eq. (20) contains no cross-product term of the type DE. This fact, which is a consequence of the orthogonality of $\hat{D}$ and $\hat{E}$, allows us to say that a certain fraction of SSS_{SCS} comes from $D\hat{D}$ and the rest from $E\hat{E}$. If, for example, D were equal to $2E$, then $D^2 = 4E^2$ and $D\hat{D}$ would account for $4/(1+4) = 80\%$ and $E\hat{E}$ for $1/(1+4) = 20\%$ of SSS_{SCS} It is the same kind of orthogonality that allowed 5% of SSS_{calcd} for the tetraiodocobaltate ion to be attributed to the ligand field (Section 2.3).

For the diagonal coefficient operators discussed here, the condition for a parameter product to vanish in

Table 1
Symmetry classification of the usual real d-orbitals

	$D_{\infty h}$	D_{4h}	D_{2h}	O_h
z^2	σ: a_{1g}	a_{1g}	a_{1g}	$e_g(\theta)$
yz	π e_{1g}(sin)	e_g(sin)	b_{3g}	$t_{2g}(\xi)$
zx	π e_{1g}(cos)	e_g(cos)	b_{2g}	$t_{2g}(\eta)$
xy	δ e_{2g}(sin)	b_{2g}	b_{1g}	$t_{2g}(\zeta)$
x^2-y^2	δ e_{2g}(cos)	b_{1g}	a_{1g}	$e_g(\epsilon)$

SSS_{SCS} is that the coefficient columns of the operators involved are orthogonal, hence the name: orthogonal operators. As an example, one may check the orthogonality of the coefficient columns of $\hat{D}$ and $\hat{E}$ that are given indirectly in Eq. (14). One may also check that the square sum of the coefficients are 400/7 for both operators. This quantity is called the norm square of the operator and its square root the norm (see below).

Had the non-orthogonal operators $\hat{C}$ and $\hat{B}$ been used, then SSS_{SCS} would have had a cross-product term containing a BC product:

$$SSS_{SCS} = \tfrac{400}{7}(D^2 + E^2) = \tfrac{700}{9} C^2 + \tfrac{3500}{9} BC + \tfrac{18550}{9} B^2 \quad (21)$$

In other words, with non-orthogonal operators, one obtains in this case three terms in the expression for SSS_{SCS} and it is no longer possible to attribute the terms to the individual parameters.

A comparison of Eqs. (20) and (21) can be had by pointing to the extended version of the Pythagorean theorem for a triangle ABC with the angles A, B, and C and their opposite sides a, b, and c. The following mathematical formula, sometimes called the cosine relations, applies to such a general triangle: $c^2 = a^2 + b^2 - 2ab \cos C$, which degenerates into the Pythagorean theorem when the angle C becomes a right angle. This situation corresponds to the orthogonal-operator situation of Eq. (20) while the extended version with cos C different from zero gives an operator overlap and a concomitant cross-product term corresponding to Eq. (21).

The fact that SSS_{SCS} has the same coefficient to D^2 and E^2 in Eq. (20) expresses the normalizing condition for $\hat{D}$ and $\hat{E}$ in the orthonormal-operators formalism.

Once the sum-square-splitting is acknowledged as an interesting quantity, the root-mean-square (RMS) splitting, which is the square root of the mean SSS and therefore has the dimension of energy, may be taken as a measure of the global splitting of the configuration d^q. We then have the definition

$$RMS = \sqrt{SSS/\text{number of states}} \quad (22)$$

with a certain analogy to the definition of standard deviation (though this may have the number of degrees of freedom in its denominator [45]). The norm of a coefficient operator is the unit chosen for the associated parameter of the corresponding parametrical Hamiltonian term. This means that the parameters D and E, which both have the norm, square root of 400/7, are commensurable so that their contributions to RMS are additive in the same way as are orthogonal vectors (Eqs. (20) and (22) and the Pythagorean expression).

Orthonormal operators have been used for pure symmetry purposes [46], for the parametrical p^q [31] and d^q models [42] and more generally in the parameterization of atomic spectroscopic data [45]. Here, we do not want to go further into the subject, except for mentioning that such concepts as norm squares and overlaps of operators are function-basis independent. It should in this context be noted that the expression for the operator overlap takes on a slightly more complicated form when a function basis is used in which the operators are non-diagonal [46,42].

In conclusion to this subsection, we recapitulate that we have used the orthonormal-operators formalism to obtain the SCS model in terms of the set of repulsion parameters $\{D, E\}$, which have a number of advantages as compared with the conventional choice of $\{F^2, F^4\}$ or $\{C, B\}$. The orthonormalization advantage has been stated in Eq. (20) and the illuminating relation between the parameters and the eigenenergies in Fig. 1.

3.2. The Slater–Condon–Shortley model (SCS) adapted to Kohn–Sham DFT

We saw in Section 3.1 that the SCS eigenstates of d^q gaseous ions have the total S and L well-defined. KS-DFT does not allow picking out functions with well-defined S and L, except in special cases. Thus, the calculated energies may not correspond to eigenstates of a spherically symmetrical Hamiltonian. As it will be

further commented on in Section 4.1, what we shall aim at calculating directly by ADF is the energy associated with single Slater determinants, set up in the usual real d-orbital basis.

This basis, further characterized in Table 1, is simultaneously symmetry-adapted to the hierarchies

$$R_{3i} \supset O_h \supset D_{4h} \supset D_{2h} \quad (23)$$

$$R_{3i} \supset D_{\infty h} \supset D_{4h} \supset D_{2h} \quad (24)$$

In this form real orbitals have been used [47,48] to establish sign-fixed Clebsch–Gordan coefficients for all the groups involved in Eqs. (23) and (24) where R_{3i} represents the three-dimensional rotation-reflection group.

Since the interelectronic repulsion is a pair interaction, the configuration d^2 is of special importance. The Slater determinants of this configuration fall into three classes.

In the highest-energy class, class 0, there are two electrons in the same orbital. This class, which embodies only five of the 45 states, is unique by all its states being degenerate. Its parametrization is detailed in Table 2, in which the first three columns of the numerical results are equivalent to the Eqs. (25), (27) and (29). The energy of class 0 only depends on D when it is measured relative to the average energy of the d^2 configuration $H_{\text{av.}}(d^2)$. The Pauli principle requires the spins of the two electrons to be opposite so that $M_S = 0$.

When the two electrons occupy different orbitals, still with $M_S = 0$, we have the class of next highest average energy, class 1 (Table 2). This class has four sub-classes,

Table 2
The SCS coefficient operators acting on d^2 determinants and the primary ADF PW91 calculations on the d^2 system, V^{3+}

		$\hat{H_{\text{av.}}}$	$21\hat{D}$	$21\hat{E}$	Computed/μm^{-1}	Predicted/μm^{-1}
J_0	$(z^2, \alpha)(z^2, \beta)$	1	40	0	0.777932	0.654771
	$(xy, \alpha)(xy, \beta)$	1	40	0	0.757943	0.654771
	$(yz, \alpha)(yz, \beta)$	1	40	0	0.754174	0.654771
	$(zx, \alpha)(zx, \beta)$	1	40	0	0.754174	0.654771
	$(x^2-y^2, \alpha)(x^2-y^2, \beta)$	1	40	0	0.754167	0.654771
$J_{\delta\delta}$	$(xy, \alpha)(x^2-y^2, \beta)$	1	4	20	−0.081215	−0.026695
$J_{\sigma\pi}$	$(z^2, \alpha)(yz, \beta)$	1	4	12	−0.253774	−0.211947
	$(z^2, \alpha)(zx, \beta)$	1	4	12	−0.253774	−0.211947
$J_{\pi\pi}$ and $J_{\pi\delta}$	$(yz, \alpha)(xy, \beta)$	1	4	−4	−0.671113	−0.582452
	$(zx, \alpha)(xy, \beta)$	1	4	−4	−0.671113	−0.582452
	$(yz, \alpha)(zx, \beta)$	1	4	−4	−0.677071	−0.582452
	$(yz, \alpha)(x^2-y^2, \beta)$	1	4	−4	−0.681704	−0.582452
	$(zx, \alpha)(x^2-y^2, \beta)$	1	4	−4	−0.681704	−0.582452
$J_{\sigma\delta}$	$(z^2, \alpha)\ (xy, \beta)$	1	4	−12	−0.851193	−0.767704
	$(z^2, \alpha)(x^2-y^2, \beta)$	1	4	−12	−0.862399	−0.767704
$\kappa_{\delta\delta}$	$(xy, \alpha)(x^2-y^2, \alpha)$	1	−14	30	−0.357007	−0.367428
$\kappa_{\sigma\pi}$	$(z^2, \alpha)(zx, \alpha)$	1	−14	18	−0.588966	−0.645307
	$(z^2, \alpha)(zx, \alpha)$	1	−14	18	−0.588966	−0.645307
$\kappa_{\pi\pi}$ and $\kappa_{\pi\delta}$	$(zx, \alpha)(x^2-y^2, \alpha)$	1	−14	−6	−1.140966	−1.201063
	$(yz, \alpha)(x^2-y^2, \alpha)$	1	−14	−6	−1.140966	−1.201063
	$(yz, \alpha)(zx, \alpha)$	1	−14	−6	−1.154946	−1.201063
	$(yz, \alpha)(xy, \alpha)$	1	−14	−6	−1.160921	−1.201063
	$(zx, \alpha)(xy, \alpha)$	1	−14	−6	−1.160921	−1.201063
$\kappa_{\sigma\delta}$	$(z^2, \alpha)(xy, \alpha)$	1	−14	−18	−1.396856	−1.478941
	$(z^2, \alpha)(x^2-y^2, \alpha)$	1	−14	−18	−1.406188	−1.478941

Column 1 contains the classes and subclasses of the determinants, whose individual members are given in column 2. Class 1 (Eq. (27)) is represented by only half of its members, its $\alpha\beta$ determinants, but it comprises also the corresponding $\beta\alpha$ determinants. Class 2 (Eq. (29)) is likewise represented by half of its members, in this case by its $\alpha\alpha$ determinants, but it comprises also the corresponding $\beta\beta$ determinants. Within both classes, corresponding determinants have the same energies. Columns 3, 4 and 5 contain an illustration of the coefficient operator expressions associated with the classes and subclasses of Eqs. (25), (27) and (29). Column 6 shows the primary ADF PW91 energies and column 7 the predicted energies based upon the secondary ADF results. These results are $H_{\text{av.}}(d^2) = -0.617(11)\ \mu m^{-1}$, $D = 0.668(15)\ \mu m^{-1}$, and $E = 0.486(20)\ \mu m^{-1}$ obtained by a least squares fitting of the 45 equations to the form of the SCS model given in Eq. (15) using the energy expressions and the primary ADF results of the present table. The zero point of energy is the energy of the AOC SCF calculation (Section 4.1). The spectroscopically determined values are $D = 0.669(19)\ \mu m^{-1}$ and $E = 0.465(17)\ \mu m^{-1}$ and also here, the standard deviations refer to the least squares data reduction rather than the experimental uncertainties.

which in order of decreasing energy may be designated $\delta\delta$, $\sigma\pi$, $\pi\delta + \pi\pi$ and $\sigma\delta$, respectively (Table 1). When the spins are permuted, it is seen that this class has 20 elements.

The last and lowest-energy class, class 2 (Table 2), has the determinants with $M_S = 1$ and -1 (Table 2 $M_S = 1$). This last class contains the remaining 20 determinants of d^2, so that the three classes together embody all the 45 states of d^2 (Eq. (14)).

The energy of class 0 is equal to the unique Coulomb integral, which, when using $H_{av.}(d^2)$ as the zero point of energy, obtains the parametrical expression:

$$J_0 \equiv \left\langle \psi(1)\psi(2) \left| \frac{1}{r_{12}} \right| \psi(1)\psi(2) \right\rangle = \frac{40}{21} D \tag{25}$$

where ψ is any real d-orbital (Table 1).

The energies of class 1 are also equal to J integrals. However, these are integrals connecting a pair of different orbitals. $J_{\pi\pi}$ is, for example, given by:

$$J_{\pi\pi} \equiv \left\langle zx(1)yz(2) \left| \frac{1}{r_{12}} \right| zx(1)yz(2) \right\rangle \tag{26}$$

The energies of class 1 are:

$$J_1 = J_{\delta\delta} = \tfrac{4}{21} D + \tfrac{20}{21} E \tag{27}$$
$$J_2 = J_{\sigma\pi} = \tfrac{4}{21} D + \tfrac{12}{21} E$$
$$J_3 = J_{\pi\delta} = J_{\pi\pi} = \tfrac{4}{21} D - \tfrac{4}{21} E$$
$$J_4 = J_{\sigma\delta} = \tfrac{4}{21} D - \tfrac{12}{21} E$$

The energies of class 2 are differences between corresponding J and K integrals where, for example,

$$K_{\pi\pi} \equiv \left\langle zx(1)yz(2) \left| \frac{1}{r_{12}} \right| yz\,(1)zx\,(2) \right\rangle \tag{28}$$

The expressions are:

$$\kappa_1 \equiv J_1 - K_1 = -\tfrac{14}{21} D + \tfrac{30}{21} E \tag{29}$$
$$\kappa_2 \equiv J_2 - K_2 = -\tfrac{14}{21} D + \tfrac{18}{21} E$$
$$\kappa_3 \equiv J_3 - K_3 = -\tfrac{14}{21} D - \tfrac{6}{21} E$$
$$\kappa_4 \equiv J_4 - K_4 = -\tfrac{14}{21} D - \tfrac{18}{21} E$$

As can be observed from the coefficients to D and E, $\hat{D}$ distinguishes between classes while $\hat{E}$ distinguishes between subclasses. However, for $D/E = 3/2$, which is a good average for the spectroscopically known parameter values, classes 2 and 3 are energywise intertwined.

The application of the pair-interaction model to the other d^q determinants may be illustrated by one rather general example for which the d^4 determinant given in Eq. (30) has been chosen

$$\left|(z^2, \alpha)(zx)^2(xy, \alpha)\right| \tag{30}$$

There are $\binom{4}{2} = 6$ pairs of spin–orbitals, one belonging to the J_0 class, two to the J class, and three to the κ class. More specifically the energy associated with the determinant is

$$J_0 + J_2 + J_3 + \kappa_2 + \kappa_3 + \kappa_4 \tag{31}$$

when Eqs. (25), (27) and (29) are used together with Table 1. The expression of Eq. (31) can be contracted into a sum of D and E terms using the same equations.

3.3. Importance of the distinction between S and M_S: eigenenergies, spin flip, symmetry restrictions, and SCS restrictions upon KS-DFT energies

This last subsection summarizes the theoretical essentials of the present paper.

Let us begin the discussion by noting (Table 2) that there is a 1:1 relation between pairs of determinants of classes 1 and 2, which individually may be labeled by well-defined absolute values of M_S (class 1: $M_S = 0$; class 2: $|M_S| = 1$) while only class 2 has a well-defined value of S, $S = |M_S| = 1$. An individual determinant from a given class is invariably related to one from the other by a spin flip of one electron. For example, the spatial pair $\{(yz), (zx)\}$ provides the pair of class 1 determinants, $\{|(yz, \alpha)(zx, \beta)|, |(yz, \beta)(zx, \alpha)|\}$, and the corresponding pair of class 2 determinants, $\{|(yz, \beta)(zx, \beta)|, |(yz, \alpha)(zx, \alpha)|\}$. Any of these four determinants have the property that the sign change of the m_s value of one of the spin–orbitals of the determinant, i.e. $\alpha \rightarrow \beta$ of one fixed spatial orbital or $\beta \rightarrow \alpha$, will transform this determinant into one of those taken from its corresponding pair of the other class. In other words, a spin flip is a change of M_S rather than S. Since S rather than M_S is a good quantum number for a spin-free Hamiltonian, the concept of a spin flip is of limited usefulness and often likely to cause confusion. The concept applies to single determinants, but if a spin flip happens to an eigenstate given by a single determinant, the resulting state, which necessarily has $\Delta M_S = \pm 1$ will not be an eigenstate with $\Delta S = \pm 1$. Moreover, it should be noted that a spin flip is Pauli-principle forbidden for doubly occupied orbitals, e.g. for the class 0 determinants, and therefore cannot involve these.

As we shall see in Section 4, KS-DFT in general and ADF in particular, naturally dictates us to focus on well-defined M_S rather than well-defined S. Therefore, our classes and subclasses have been chosen so as to have well-defined M_S and thereby to be directly adapted to KS-DFT. ADF allows us to calculate energies that may be interpreted as the expectation values of the repulsion operator with respect to all the 45 determinants of Table 2 [49]. If class 0 is also counted as a subclass, we have nine subclasses of energy quantities altogether. We shall talk about a nine-parameter model (Table 3) in spite of the fact that it involves only eight

Table 3
Nine-parameter model of the d^2 configuration

	Weights	$21\hat{D}$	$21\hat{E}$	Predicted/μm^{-1}	Differences	Calculated/μm^{-1}	Differences
J_0	5	40	0	0.655		0.760	
$J_{\delta\delta}$	2	4	20	−0.027		−0.081	
					0.185 ≈ 1		0.173 ≈ 0.82
$J_{\sigma\pi}$	4	4	12	−0.212		−0.254	
					0.370 ≈ 2		0.423 ≈ 2
$J_{\pi\pi}$ and $J_{\pi\delta}$	10	4	−4	−0.582		−0.677	
					0.186 ≈ 1		0.180 ≈ 0.85
$J_{\sigma\delta}$	4	4	−12	−0.768		−0.857	
$\kappa_{\delta\delta}$	2	−14	30	−0.367		−0.357	
					0.278 ≈ 1		0.288 ≈ 1.02
$\kappa_{\sigma\pi}$	4	−14	18	−0.645		−0.589	
					0.556 ≈ 2		0.563 ≈ 2
$\kappa_{\pi\pi}$ and $\kappa_{\pi\delta}$	10	−14	−6	−1.201		−1.152	
					0.278 ≈ 1		0.250 ≈ 0.89
$\kappa_{\sigma\delta}$	4	−14	−18	−1.479		−1.402	

The first column gives symbols for the energy subclasses. The second column their weights. The third and fourth columns indicate the diagonal elements of $\hat{D}$ and $\hat{E}$. The fifth and seventh ones give the predicted and calculated ADF-PW91 sub-class energies using the D and E values of Table 2 for the prediction. Columns six and eight give subclass energy differences and their ratios which should be 1:2:1 for symmetry reasons. It should be noted that the predicted and calculated energies may differ by as much as 0.1 μm^{-1}.

independent energy differences. If $H_{av.}(d^2)$ is chosen as the zero point of energy, i.e. $H_{av.}(d^2) = 0$, the weighted sum of the nine parameter values is equal to zero. By the same token, we shall talk about two entirely different three-parameter models. One is the class model, which involves the three class energies, J_0, $J_{av.}$, and $\kappa_{av.}$, and which–because of Eqs. (27) and (29) and their internal weights (Table 3)—does not provide information about the parameter E. The other three-parameter model is the SCS model, which involves $H_{av.}(d^2)$ as an explicit parameter in addition to the parameters D and E.

Finally, we focus on the results of the energy expressions of Eqs. (25), (27) and (29), which are reproduced in a different form in Tables 2 and 3 . Thus, we look at the 45 states of the configuration d^2, described in a Slater determinantal basis of real orbitals. We shall distinguish between the symmetry restrictions, which, if class 0 is regarded to be its own subclass, are subclass properties, and the SCS restrictions, which are inter- and intraclass properties. Taken together, they allow the 45 expectation values of the energy of d^2 to be reduced to the three parameters $H_{av.}$ (d^2), D and E of the SCS model.

Concerning the symmetry part, there is an intra-subclass and an intersubclass restriction. If again class 0 is regarded to be its own subclass, then the intra-subclass restriction is contained in the statement that the energies are subclass properties: each subclass has its own characteristic energy, thereby reducing the 45 expectation values to the nine-parameter model, mentioned above. The intersubclass restriction can be read out of the coefficients to the parameter $\boldsymbol{E}$. These reveal that the three energy differences between the four consecutive subclasses of class 1 as well as class 2 stand in the ratio 1:2:1 to each other.

Concerning the SCS part, there are two numerical interclass restrictions, one associated with the parameter $\boldsymbol{E}$ and one with D. The E restriction is revealed by comparing classes 1 and 2, and observing that the energy splitting is 50% higher in class 2 than in class 1. The D restriction can be expressed as:

$$J_0 - J_{av.} = 2(J_{av.} - \kappa_{av.}) = \tfrac{36}{21} D \tag{32}$$

where av. may be replaced by the subclass numbers 1, 2, 3, or 4 (Table 3 and Eqs. (27) and (29)) as a consequence of the SCS restriction on E.

The two symmetry restrictions and two SCS restrictions, just described for the SCS model, will be important for the comparison between the ADF results and the SCS results to be discussed in Section 4.3 (especially Eq. (34)).

4. KS-DFT in the form of ADF

4.1. Preliminaries of KS-DFT: occupation numbers of spin–orbitals

In DFT the starting point fundamentally is the electronic density distribution $\rho(r)$. ADF, however, is based on the Kohn–Sham (KS) orbital concept. Here the basic quantities are a set of orthonormal spin–orbitals combined with their individual occupation num-

bers ($0 \leq n \leq 1$). The components of the total energy are functionals of other quantities that are derivable from the spin–orbitals and their occupations. For example, the Coulomb energy is a functional of the total electronic density distribution, whereas the exchange-correlation energy is a functional of the distribution of the electrons with α and β spins, separately.

The ADF program does not require the occupation numbers to be integers. To the contrary, the authors recommend that one starts with the average of configuration (AOC) input when the ground state is orbitally degenerate [6,50]. This means that the first calculation one makes with a d^3 system, say, is one in which the occupation numbers of the inner shells are unity for all spin–orbitals while they are 3/10 for the 10 spin–orbitals of d type. This procedure is very attractive for our purpose since a self-consistent field calculation (SCF) on this basis will provide us with an R_3 adapted orbital basis for our atomic ion. In the main part of our work, these orbitals remain frozen while used for the subsequent calculations [50] on the atomic system (fixed charge z and fixed atomic number Z). By this strategy the resemblance with LFT is obvious.

We need to comment on the AOC energy. Unless the occupation numbers of the spin–orbitals correspond to a single determinant [49], that is, unless all the non-trivial occupation numbers are unity, there are problems in interpreting the energy, at least that calculated with the current exchange-correlation functionals. There is apparently no method available to correct for this. Therefore, in order to obtain energies that can be interpreted, we shall in our main text only use energies associated with occupation numbers of unity. Thus, the SCF energy of the AOC calculation is not in itself useful for our present purpose, and it will not be used until the Appendix. In the main text, the AOC energy only serves as an external zero point of energy, the internal one being either that of one of the eigenstates of the system in question or the average energy calculated for the whole configuration (Fig. 1) or a well-defined part of it (Section 4.3). Notably, the AOC energy is not the average energy of the configuration [50] (see also Appendix). The average energy of the configuration is calculated as the average energy of the $\binom{4l+2}{q}$ real Slater determinants of d^q.

Thus, we do not use the energy calculated for the AOC. We do, however, need the orbitals defined by the AOC–SCF calculation. It should be noted that the single determinants whose energies thus form the basis of our work are not in general eigenfunctions of the operator $\hat{L}^2$, i.e. they do not have well-defined values of the orbital angular momentum L, and, therefore, they are not eigenfunctions of the Hamiltonian of our spherical atomic systems. The same holds true for the operator $\hat{S}^2$ so that the determinants do not in general have well-defined values of the total spin S. However, for $M_S = M_S\text{max}$ and $M_S = M_S\text{min}$, we have $|M_S| = S$, and all the determinants of class 2 have $S = 1$ (Tables 2 and 3 and Section 3.2).

Real orbitals seem to be fundamentally necessary since, with an example from the d^2 configuration, the two determinants $|(2, \alpha)(1, \alpha)|$ and $|(2, \alpha)(-1, \alpha)|$ determine the same density distribution of d-electrons with α spin and thereby have the same ADF energies, but actually must have different energies, as $|(2, \alpha)(1, \alpha)|$, is a neat ^3F function, while $(2, \alpha)(-1, \alpha)|$ is a mixture of 40% ^3P and 60% ^3F.

The KS d-spin–orbitals are eigenfunctions of the KS one-electron energy operator. The physical meaning of these orbitals has been debated [51]. In this work we use the KS d-orbitals in a pragmatic and concrete way. We take the d orbitals provided by the AOC calculation and use the energies of the density distributions defined for α and β electrons by the individual Slater determinants built from these orbitals as the link between ADF and ligand-field theory, thus testing the assumption that these KS d-orbitals make up a reasonable basis for ligand-field theory.

Our assumption is that the energy we calculate for a given real determinant corresponds to what is usually called the expectation value of the Hamiltonian with respect to this determinant.

Finally, we note that the fact that the AOC orbitals are used for both α and β spin means that all our calculations are restricted in the Hartree–Fock sense even though a calculation concerning for instance class 2 of d^2 (Table 2) must be called unrestricted in the ADF input.

4.2. The primary and secondary links between ADF and the SCS part of ligand-field theory

In ligand-field theory in the form of the parametrical d^q model, the energy may be modeled by an effective Hamiltonian acting on a subspace of the Hilbert space with a basis given by the $\binom{4l+2}{q}$ Slater determinants. Given the relevant parameters within the model, for example Δ, B and C for an octahedral complex (Section 2.3), one can calculate the energy of any linear combination of the Slater determinants. In particular, one can calculate the energy of a multiplet term directly within this model. As an important point, this Hamiltonian is totally symmetric, that is, it has the symmetry of the given problem, by construction. In our present use of ADF, the ligand-field is zero and the symmetry is spherical. That is, we do zero-ligand-field calculations.

The link between LFT and our ADF calculations then is that we associate the expectation value of a LFT

Hamiltonian for a Slater determinant build from standard real d-spin–orbitals with the energy arrived at by the corresponding ADF calculation. In this way ADF calculations provide the diagonal matrix elements of the LFT Hamiltonian in this determinantal basis. ADF is unable to provide us with the non-diagonal matrix elements of the Hamiltonian and, therefore, we are unable to calculate the multiplet term energies directly by diagonalization.

In order to calculate the multiplet term energies, we have, in this paper, used the SCS model in the $\{D, E\}$ parametrization. As discussed in Section 3.2, the interelectronic pair interactions fall in the three classes 0, 1, and 2 whose energies have been expressed in Eqs. (25), (27) and (29), respectively, and in Tables 2 and 3. For the d^2 system, for example, these equations together with the ADF energies of the 45 determinants provide us with 45 equations for the determination of the parameters $H_{av.}$, D, and E, and the multiplet energies can then be calculated by using Eq. (14). For the general d^q configuration, there are $\binom{4l+2}{q}$ states and thereby the same number of determinants, whose energies by summation over all pairs of electrons (the pair-interaction model) can be directly expressed in terms of D and E parameters by using Eqs. (25), (27) and (29). There will be $\binom{4l+2}{q}$ pieces of information from ADF (i.e. the number of equations) to determine the parameter set $\{H_{av.}, D, \mathrm{E}\}$.

If our effective ADF energy operator acting on d^q should fully qualify as a Hamiltonian, we would require it to be totally symmetric. Since we are unable to calculate the non-diagonal elements of the Hamiltonian, and since we aim at restraining our ADF results so as to make them comply with the SCS model, our SCS test here is that the diagonal part of the Hamiltonian should comply with the contents of Eqs. (25), (27) and (29). These equations have already been discussed in some detail in Sections 3.2 and 3.3.

One might have considered to construct the ADF Hamiltonian using standard complex d-orbitals instead and have compared this d^2 Hamiltonian with 45 equations analogous to [25,27,29], but referring to a complex $\{l, m_l\}$ one-electron basis. However, as discussed in Section 4.1, we know that this procedure would fail because ADF must associate the two non-degenerate Slater determinants $|(2, \alpha)(1, \alpha)|$ and $|(2, \alpha)(-1, \alpha)|$ with the same energy.

Moreover, even though the determinants $|(2, \alpha)(0, \alpha)|$ and $|(-2, \alpha)(0, \alpha)|$ both represent the ground state $^3F(d^2)$, their ADF energies are invariably several tenths of an electron volt higher than those of their real-function-based analogs, $|(xy, \alpha)(z^2, \alpha)|$ and $|(x^2-y^2, \alpha)(z^2, \alpha)|$.

4.3. Computational results and discussion of method

On the basis of the symmetry restrictions and the SCS restrictions of Section 3.3 and the concomitant ideal Hamiltonian requirements discussed in the previous subsection, we have now used the ADF as if it were an experimental device which, apart from an additive constant of energy, was able to provide the expectation values of the SCS Hamiltonian on d^q systems with respect to all our $\binom{4l+2}{q}$ determinants. We shall call these computed expectation values our primary ADF results. Through these, we were provided with $\binom{4l+2}{q}$ equations in the three unknowns, $H_{av.}$, D and E, to obtain the secondary ADF results. This data reduction problem was solved by using the least squares method giving each determinant the same weight.

All calculations were done using the uncontracted triple zeta Slater-type-orbital basis sets distributed with the ADF package as basis set type IV. No orbitals were frozen during the AOC-SCF calculations. No relativistic term was included in the total energy functional.

The experimental results used for providing empirical D and E values were stripped of spin–orbit coupling effects by using the SCSζ model [29].

Using these procedures, the values for D and E calculated here and the spectroscopically determined values should be as comparable as possible.

For the calculations presented in the following, we have used the Perdew–Wang 91 [52] (PW91) functionals, which are the most refined ones among the combined exchange and correlation functionals built into the ADF program. PW91 belongs to the gradient-corrected (GC) functionals so-called as opposed to the local density approximation (LDA) functionals. The GC functionals contain the gradients of the local density explicitly whereas the local density functionals do not.

It has turned out that the two kinds of functionals are good for different types of calculations [53]. For our purposes we have found that the gradient-corrected functionals are superior to the local ones. This is clear from the result that when using the local density exchange functional (or exchange-correlation functionals), the exchange energy is found to be the same for all the 10 $\alpha\alpha$ Slater determinants (all the 20 determinants of class 2 (Eq. (29)). The sum of the Coulomb and exchange-correlation functionals is unable to compensate completely for this behavior as we shall now discuss further.

The results of ADF consist of a sum of energies arising from the different functionals of the chosen set of functionals, PW91 for our main calculations. The relevant ones in our present context are the Coulomb and exchange-correlation functionals, the remaining functionals giving a vanishing contribution to the energy of all the determinants as a consequence of the frozen orbitals and AOC energies serving as the external zero points for all the energy functionals of a given set.

When the Coulomb functional is used by itself, the determinantal classes 1 and 2 as well as their corresponding subclasses (Eqs. (27) and (29) and Tables 2 and 3) obtain indistinguishable energies, and the difference between the energy of class 0 (Eq. (25)) and the average energy of the class 1 (or class 2) determinants becomes determining for the parameter $D_{\text{Colu.}}$ while the energy differences within class 1 (or class 2) become determining for $E_{\text{Coul.}}$. When the exchange-correlation functional is used alone, the difference between the average energy of the class 2 determinants and the common energy of all the remaining determinants—this common energy is zero relative to the AOC energy of the exchange-correlation functional—determines $D_{\text{exch.}}$, while the energy differences within class 2 determines $E_{\text{exch.}}$. The result of such an analysis is that the two functionals obey the symmetry and the SCS restrictions independently, the Coulomb functional exactly and the exchange-correlation functional with the usual uncertainty within which the ADF program allows the calculation of the energies of determinants belonging to the same class–subclass category, i.e. 0.02 μm^{-1}. This uncertainty is the ADF uncertainty connected with what we called the intrasubclass symmetry restriction of the d^2 model (Section 3.3 and Table 2). However, the two functionals are not commensurable and, therefore, not compatible. The Coulomb functional invariably exaggerates the values of its parameters while the exchange-correlation functional provides parameter values that are low. For example, for the V^{3+} system using the PW91 exchange-correlation functional, the following values (in units of μm^{-1}) were obtained: $D_{\text{Coul.}} = 0.78$, $D_{\text{exch.}} = 0.51$, $E_{\text{Coul.}} = 0.57$, $E_{\text{exch.}} = 0.27$. It is seen that even with this GC functional, the exchange-based parameter values are low.

When the total energies are used, the obedience toward the symmetry restrictions remains unaltered, but that toward the SCS restrictions decreases considerably. Nevertheless, the resulting parameter values based upon the least squares fitting, are surprisingly satisfactory in view of the comparatively extremely small computations involved when the ADF program is used.

In order to accentuate the difference between the LDA and GC exchange-correlation functionals, we have also calculated the spatial parameter E from the $\alpha\alpha$ determinants of d^2 (class 2, Section 3.2). The parametrical d^2 Hamiltonian for only α spin–orbitals can be expressed as [45]

$$\hat{H} = [H_{\text{av.}}(M_S = 1)]\,[\hat{H_{\text{av.}}}(M_S = 1)] + E_1\hat{E_1} \tag{33}$$

where the E parameter has been provided with a subscript 1 for $S = 1$. For V^{3+} we find the following results for E_1 using combinations of functionals normally used in the literature as provided by the ADF package: Three gradient corrected exchange-correlation functionals Becke Perdew 0.477 μm^{-1} (+5%), PW91 0.469 μm^{-1} (4.0%) and Becke LYP 0.498 μm^{-1} (10.3%) and one local functional VWN 0.379 μm^{-1}(−16.0%). Comparison with the experimental value of $E_1 = 0.452$ μm^{-1} is given in parentheses. We observe that the three GC functional sets give E values that are slightly high while the LDA functional set gives a value which is low. The parameter E_1, has a special interest because of its responsibility for the nephelauxetic series, which was mainly established on the basis of the spin-allowed ligand-field transitions of Ni(II), Cr(III), Co(III), Rh(III) and Ir(III) complexes (Section 2.3)[38].

We now go into some detail with an example which is typical of our work. With reference to subsections Sections 3.2 and 3.3, we take as an example of the use of ADF PW91 calculations the results for the d^2 system V^{3+}, which were given in Table 2. The first thing to notice about the numerical ADF and the parametrical SCS results is that the energies of the subclasses, which should be identical in SCS, turn out to deviate maximally 0.02 μm^{-1} from each other in ADF. We have already associated this deviation with the exchange-correlation functional. In order to study the other symmetry restriction discussed in Section 3.3, the results of the nine-parameter model, which involves the subclass energies as parameters, were given in Table 3. The ratios between the subclass energy differences are seen to comply reasonably well with the symmetry ratios 1:2:1. It is beyond the scope of the present paper to discuss further the double function of the coefficient operators $\hat{D}$ and $\hat{E}$ (Fig. 1). However, we would along the same lines like to point out that ADF PW91 invariably calculates energies of classes 0 and 2 determinants high and accordingly those of class 1 low. This means that it is necessary in order to obtain a representative set of calculations to include determinants from all three classes. We have chosen to attain this here by including all possible determinants and use the complete set of energies for determining the secondary ADF results, i.e. the calculated D and E parameters.

A way of accentuating the deviations between the ADF-calculated energies and those restricted by the SCS model is that of rewriting the condensed results contained in Eq. (32) in four independent equations:

$$J_0 = J_i + 2K_i = 3J_i - 2\kappa_i \quad (i = 1, 2, 3, 4) \tag{34}$$

where the left hand side refers to class 0 (Eq. (25)) whereas the two right hand side terms most to the right refer to classes 1 and 2, respectively (Eqs. (27) and (29)). The numerical ADF values referring to both sides of the four equations, valid for V^{3+}, can be taken from Table 3 directly, i.e. with AOC as the zero point of energy. The left hand side has the value $J_0 = 0.76\ \mu m^{-1}$ and the four right hand sides obtain the values 0.47, 0.42, 0.27, and 0.23 μm^{-1}, respectively, where we note the quite considerable discrepancies. In particular, we note the low values of all the right-hand side energies, a fact which most likely can be taken as evidence for an underestimation of the exchange energy. The results could, of course, alternatively be interpreted as an overestimation of J_0, which refers to the energies of the states with doubly occupied orbitals. Despite these discrepancies between the individual determinantal energies calculated by the ADF, the D and E values obtained as our secondary ADF results are considerably closer to experiment than are those obtained from open shell Hartree–Fock calculations. Moreover, the difference between calculations and experiments is less systematic. In Jørgensen's analysis [54], the Hartree–Fock values are round-about 20–25% high, not much different from the results using the Coulomb functional alone. The ADF using the present way of averaging the results calculates the spatial energy parameters E high for most, but not all systems, whereas it calculates the spin-pairing energy parameters D low for the higher oxidation states. The results have been collected together in Fig. 2, where it should particularly be noted that many of the low oxidation state ions do not have a d^q configuration as their ground states. This means that we have in these cases been concerned with an excited configuration in the calculations as well as in the spectroscopic analysis that lies behind the empirical parameter values.

Daul has presented a symmetry-based method not unlike the present one, and for the determination of energy quantities equivalent to $H_{av.}(d^2)$, D, E, he chose three determinants arbitrarily. Incidently, by his choice of determinants, class 1 (Eq. (27)) does not become represented [55].

We need to say a few words about SCF calculations. An SCF calculation on the ground state for a d^2 configuration would involve, for example, the determinant $|(z^2, \alpha)(x^2 - y^2, \alpha)|$ (Table 2) belonging to ${}^3A_{2g}(O_h)$ and with spatial electronic density distribution and thereby effective potential of octahedral symmetry. Doing this calculation as an SCF calculation in this symmetry, i.e.with the orbital restrictions of the O_h point group, thereby allowing the two d-orbitals to become more general $e_g(O_h)$ orbitals, lowers the energy by only 0.01 μm^{-1} in the case of V^{3+}. Moreover, the other determinants of d^2 give different symmetries of the effective potential and will thus allow different modifications of the d-orbitals. Moreover, for the spherical spin-polarized ion, i.e. for V^{3+} using the occupation numbers 0.4 for all the d-orbitals with α spin, the result of an SCF calculation is an energy lowering of only 0.005 μm^{-1} relative to the energy obtained using the frozen AOC orbitals. These small energy lowerings contribute to our confidence in the usefulness of our method of using frozen orbitals rather than SCF orbitals in mimicking ligand-field theory. Finally, we want to mention that the ADF does not allow the output orbitals from an SCF spin-polarized calculation to be used for subsequent calculations.

The problem of choosing ground state energies for first row transition metal atoms, i.e. $z = 0$, using KS-DFT in the form of the ADF package has previously been addressed by Baerends et al. [50]. These authors found that for Sc, a d^1 system, the ADF energies of the five real d-orbitals were satisfactorily comparable whereas this was not the case with the five complex d-orbitals. This result concerning complex d-orbitals points in the same direction as ours. These authors do not, however, reach the conclusion that complex d-orbitals are inapplicable with exchange-correlation functionals using densities based on occupation numbers of spin–orbitals as their input. Baerends et al. in fact recommend using SCF calculations on complex determinants in $D_{\infty h}$ symmetry when calculating the ground states.

5. Conclusions

We have demonstrated the usefulness of a rather special way of using density functional theory through ADF. The concept of Kohn–Sham eigenorbitals of a whole d^q configuration has been introduced as those obtainable from the AOC SCF calculation. From these eigenorbitals we have calculated the energies associated with the determinants of the d^q configurations without doing SCF calculations, i.e. using not only a frozen core, but also frozen d-orbitals, thereby mimicking ligand-field theory. This is a tough restriction from a fundamental point of view [56] since the resulting model disobeys the virial theorem [32].

Nevertheless, we have computationally obtained values of the empirical interelectronic repulsion parameters of ligand-field theory for the $3d^q$ gaseous ions in good agreement with experiment.

There are several advantages in not doing SCF calculations on the Slater determinants themselves. First, if the symmetry of the effective potential were lower than the spherical symmetry of our system, the d-orbitals would cease to be d-orbitals. Secondly, it is clearly advantageous for the mimicking of LFT to treat the ground state and the excited states within the same characterizing configuration on an equal footing.

Even though the ADF requires our use of it to be labeled ADF-unrestricted calculations since some of our determinants have $M_S \neq 0$, that is, are spin-polarized, the fact that we use frozen orbitals based upon an ADF restricted calculation, that is, the AOC calculation, has the consequence that our calculations remain restricted in the Hartree–Fock sense. Thus, our special use of ADF conserves the concept of orbitals (even if they are Kohn–Sham orbitals), which allows the normal chemical ideas of orbital energies and of excitation of electrons between orbitals rather than confusing this by using different spatial orbitals for corresponding spin–orbitals. To our knowledge, even though different orbitals for different spins have significant computational and even modeling [57,58] advantages, the chemical and, in particular, conceptual usefulness have yet to be demonstrated.

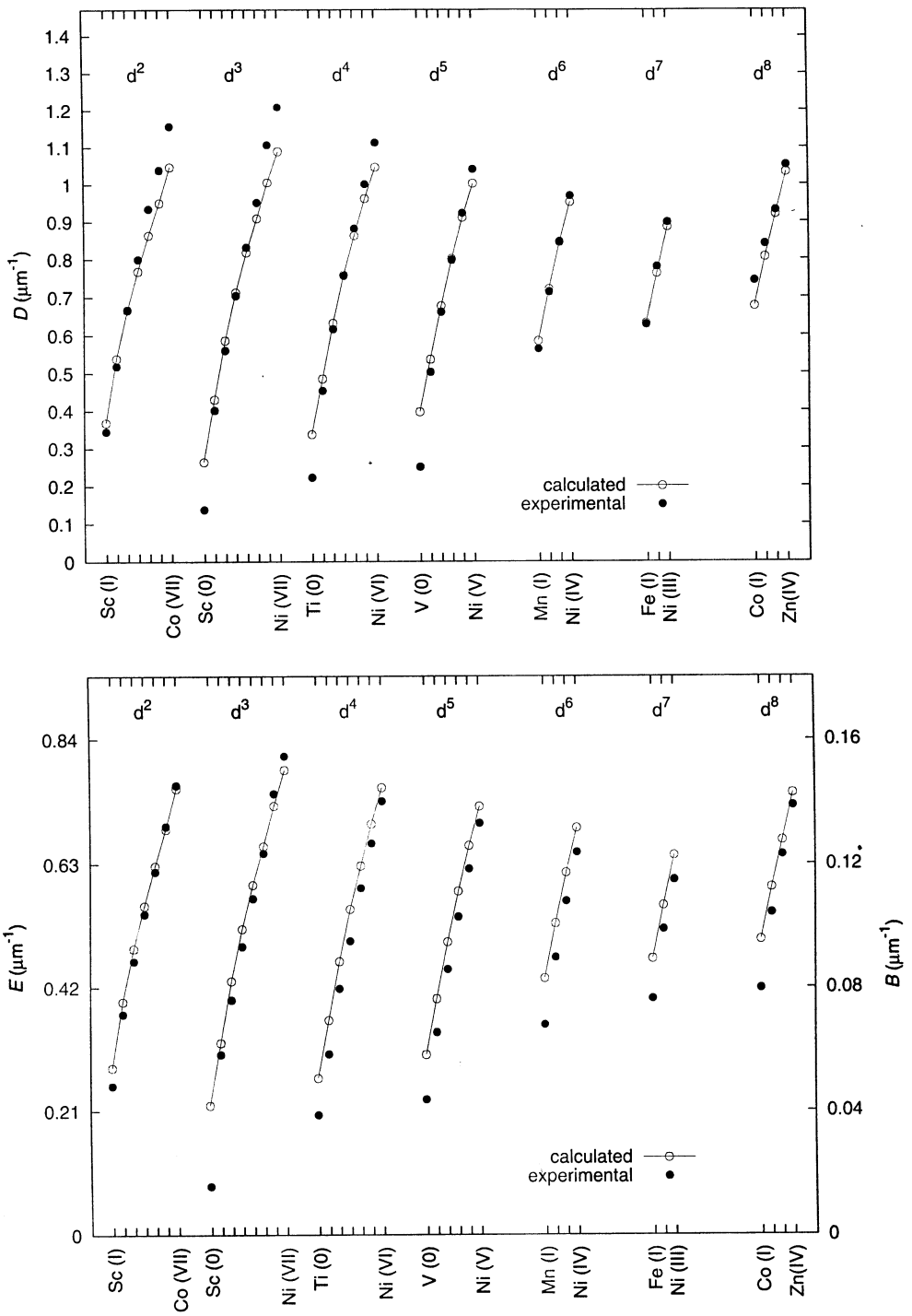

Fig. 2. Numerical results for the parameters D and E of the SCS model.

Once we have mimicked the parametrical d^q model and computationally obtained values for its empirical parameters, then we are able to calculate all its matrix elements including its non-diagonal ones. This means that we can calculate the linear combinations of our basic Slater determinants that are the eigenfunctions, which are symmetry adapted to our Hamiltonian with respect to both space and spin.

We have approached the symmetry dilemma of DFT as it is expressed by the KS-DFT of the ADF package. The inability to calculate the non-diagonal elements of the KS-DFT Hamiltonian has made it necessary to explore the symmetries of the diagonal elements in a determinantal basis of real orbitals, because complex orbitals were found to be unusable.

The way in which the SCS model reduces the 45 energies of the d^2 states to three parameters has been analyzed (Section 3.3). It was found that the restrictions required could be divided into two pure symmetry restrictions and two special SCS restrictions. Then, by comparing all these restrictions with the ADF computational results for the Coulomb and the exchange functionals independently, it was found that the two functionals are both faithful to the full SCS model, the Coulomb functional exactly, the exchange-correlation functional within the limits of its small deviations from the symmetry restrictions (ca. 0.02 μm^{-1}). However, the Coulomb functional invariably gives higher numerical values for the two SCS parameters, D an E, than does the exchange-correlation functional. Thus, the two functionals are incompatible. By adding the results from the two functionals, it is possible to see that the total ADF obeys the symmetry restrictions much better than it does the SCS restrictions. Thus, the low energy separations found for the calculated exchange-correlation energies does not seem to be mainly related to the way symmetry is handled (Section 4.3). Even though the energies associated with the individual determinants may show a deviation of more than 0.1 μm^{-1} between their ADF values and their SCS values, the parameters D and E determined by the least squares procedure obtain standard deviations of about 0.02 μm^{-1} (Table 2).

In a forthcoming paper we shall be able to exemplify similar symmetry checks within a more general d^q model, based upon the pair-interaction model that uses four independent parameters for the characterizing configuration d^2, i.e. the five parameter model when the average energy of the d^2 configuration is included. These parameters represent in essence the five energies of the multiplet terms of Eq. (14). Fig. 1 has already illustrated the four independent energy differences and the double function of $\hat{D}$ and $\hat{E}$ of the Slater–Condon–Shortley model.

In conclusion, we calculated the values of the interelectronic repulsion parameters D and E of the SCS model. Thus, we obtained computationally the denominator of Eqs. (3) and (4), which are the numbers required in order to be able to calculate the nephelauxetic quotient. The next step is, of course, to obtain the numerator computationally. This will be our next project. With most of the existing computational models, this would have been a formidable ambition, but with KS-DFT—if the problem can be properly formulated—the chances are that the calculations themselves will be comparatively manageable.

Acknowledgements

Our inspiration came from Jesper Bendix and indirectly from R.J. Deeth, who used ADF for describing the bonding in a new series of d^1 and d^2 nitrido complexes of the first transition series [2]. We are also indebted to Tom Ziegler and Michael Atanasov who at an early stage of this work encouraged us to pursue it. We are pleased to acknowledge the participation of Jesper Bendix and Michael Brorson in the parametrization of the experimental data in connection with earlier work [45]. C.A. acknowledges the financial support from Kemisk Instituts rejseudvalg and Acta Chem. Scand. as well as an Elsevier Golden Jubilee Bursary allowing him to communicate the present results at the 34th ICCC in Edinburgh. Acta Chem. Scand. has also supported the participation of C.S. in the XIIth Winter School on Coordination Chemistry held in Karpacz, Poland, in December 2000 and the Carlsberg Foundation his attendance of the 50 years anniversary of the coordination chemistry section of the Japanese Chemical Society and the international symposium in this connection, both held in Kusatsu, Japan in September 2000.

Appendix. Use of energies of spin-polarized, spherical densities corresponding to M_S values of S_{max}, $S_{max}-1$, …, S_{min}

As mentioned in Section 4.1, Kohn–Sham DFT should represent Slater determinants with a well-defined value for M_S when the occupation numbers for the spin–orbitals are restricted to being either zero or unity, and under these circumstances one should be able to calculate an energy quantity corresponding to the expectation value of the Hamiltonian with respect to this determinant. The energy considerations of the main part of this review are based upon this limitation on occupation numbers.

However, the 3d-orbitals were defined by doing an SCF calculation, so-called the average of configuration calculation (AOC), where the occupation numbers for a d^q configuration are $q/10$ so that the q electrons are equally distributed upon the 10 spin–orbitals. This

distribution has spherical symmetry of its electronic density, but nevertheless its energy does not correspond either to a well-defined quantum mechanical state (for d^2 for example the ^1S state) or to the average energy of the configuration calculated as the average energy of the $\binom{4l+2}{q}$ states. An obvious question then is: can the energy of AOC be interpreted? If it is possible, then this spatially spherical Kohn–Sham state cannot be anything but a mixture of states. Therefore, the first assumption might be that the value of M_S is well-defined for AOC, i.e. $M_S = 0$ for q even. Then, what about q odd? These considerations lead to the question as to whether other spatially spherical Kohn–Sham states have well-defined values of the absolute value of M_S. Within our limited scope of studying the SCS model, these assumptions can be tested operationally by simply applying ADF to such situations, again focusing mainly upon energy differences. We have done this by calculating the energies corresponding to all possible $|M_S|$ values for each d^q configuration, and by using the AOC orbitals as well as by doing SCF calculations.

In order to proceed, a SCS analysis of the average energy of spatially spherical states with definite values of M_S is necessary. We do this by way of an example: the d^2 configuration. From Eq. (14) we note that all the spatial states, $(2L+1)$ for each multiplet term, may be combined with $M_S = 0$ so that there are 25 states with $M_S = 0$ (class 0 + class 1, Eqs. (25) and (27)). We are left with 20 states whose absolute value of M_S is equal to unity (class 2, Eq. (29)). It is immediate that the average energies, $H_{av.}$ $(M_S = 0)$ and $H_{av.}$ $(M_S = 1)$, are independent of the spatial energy parameter E (Fig. 1). By using Eq. (14) leaving out $H_{av.}(d^2)$, we obtain the results

$$25H_{av.}(M_S = 0) = 10\,(\tfrac{-14}{21})\,D + 1\,(\tfrac{112}{21})\,D + 14\,(\tfrac{22}{21})\,D = \tfrac{40}{3}\,D \quad (A.1)$$

$$H_{av.}(M_S = 1) = -\tfrac{2}{3}\,D \quad (A.2)$$

and the formula needed for our purpose,

$$H_{av.}(M_S = 0) - H_{av.}(M_S = 1) = \tfrac{6}{5}\,D \quad (A.3)$$

is to be compared with Eq. (18) and with the discussion of subsection Section 3.3 and Fig. 1. The formula Eq. (A.3) can be generalized to the following one, valid for the higher M_S value, M_S^{high}, being one higher that the lower one.

$$\frac{H_{av.}(M_S^{high} - 1) - H_{av.}(M_S^{high})}{2M_S^{high} - 1} = \frac{6}{5}\,D \quad (A.4)$$

Formulas similar to Eq. (A.4) have been obtained by Slater and Jørgensen [34,59].

We have now calculated the energies of the spatially spherical states with all the M_S values relevant to d^q configurations for all q. For a d^2 configuration we have calculated the energies for two different sets of occupation numbers; one set coincides with the occupation numbers of AOC and corresponds to $M_S = 0$. The other set has occupation numbers equal to 0.4 for the five α d-spin–orbitals and 0 for the β spin–orbitals,

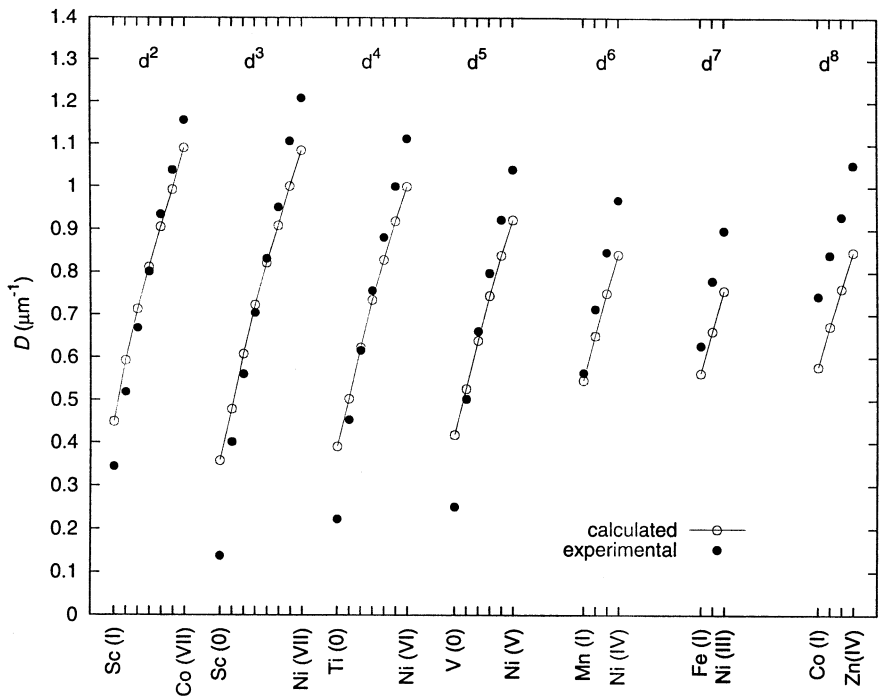

Fig. 3. Spin-pairing energy parameters D, calculated for spherical electronic densities.

Table 4

d^5			Un-converged		Converged
$\lvert M_S\rvert = \frac{5}{2}$	$H_{av.}(d^5) - \frac{140}{21} D$		-5.580		-5.630
		$4.8D$		3.583	
$\lvert M_S\rvert = \frac{3}{2}$	$H_{av.}(d^5) - \frac{196}{5.21} D$		-1.997		-2.019
		$2.4D$		1.776	
$\lvert M_S\rvert = \frac{1}{2}$	$H_{av.}(d^5) - \frac{56}{5.21} D$		-0.221		-0.224

and thus corresponds to $M_S = 1$. In both cases the AOC orbitals are used. We have calculated the same energy quantities using a SCF operation with almost the same results.

The results obtained show reasonable values for the spin-pairing energy parameter D. They are pictured graphically in Fig. 3 together with those known from atomic spectroscopy. The figure should be compared with the earlier figure, Fig. 2. It is then seen that the present method gives results of comparable quality for lower values of q. For high values of q as well as for high and low charges the method used in Fig. 2 generally gives better results.

Noting that d^4, d^5 and d^6 configurations embody three different M_S values and thereby two independent energy differences, let us dig a little deeper into the calculated results.

We take $Fe^{3+}(d^5)$ (Table 4) as our example. The table contains the frozen-orbital calculations (called, with ADF, un-converged) referred to earlier as well as the SCF ones (called converged). We see that even in the $M_S = 5/2$ calculation where one would expect the largest effect of SCF convergence, the energy lowering is moderate. From the example we also note that the calculations follow Eq. (A.4) very closely. The energy differences provide us with two determinations of D that differ by less than 1%, but are 7% low relative to the experiment (0.798(3) μm^{-1}) [29]

$$D = \frac{3.583\ \mu m^{-1}}{4.8} = 0.746\ \mu m^{-1} \qquad (A.5)$$

$$D = \frac{1.776\ \mu m^{-1}}{2.4} = 0.740\ \mu m^{-1}$$

It is noteworthy that D can be calculated equally satisfactorily in two independent pairs of calculations in the case of all the d^4, d^5, and d^6 configurations.

Recalling the contents of Table 3, we are able to calculate $H_{av.}$ ($M_S = 1$) and $H_{av.}$ ($M_S = 0$) for a d^2 system, here V^{3+} in a different way. $H_{av.}$ ($M_S = 1$) is the weighted average energy of the κ class (Eq. (29)), the class 2 determinants, and thus equals -1.010 μm^{-1}. $H_{av.}$ ($M_S = 0$) is the average energy of the J classes, class 0 (Eq. (25)) and class 1 (Eq. (27)), and thus equals -0.303 μm^{-1} For comparison, the values calculated with the method in this appendix is -0.856 μm^{-1} for $M_S = 1$ and 0.000 (the energy corresponding to AOC) for $M_S = 0$. Since all our calculations share the same zero point of energy, the energy of the AOC, the energy values given are pairwise directly comparable. This fact allows us to conclude that the method presented here and the one of the main text should not be used together.

The D value which is calculated from the differences between the average energies of the J and κ classes using Eq. (A.3) is $(1.010–0.303)$ $\mu m^{-1}/1.2 = 0.589$ μm^{-1}. This value differs significantly from the D value calculated by the least-squares-method in the main text, which is 0.668 μm^{-1} (Table 2). This discrepancy is caused by the deviations from the SCS model described in Section 4.3 and in the caption to Table 3. The value calculated for D in this appendix is 0.713 μm^{-1} and the experimental value is 0.669 μm^{-1} [29].

References

[1] R.J. Deeth, Structure and Bonding 82 (1995) 1.
[2] J. Bendix, R.J. Deeth, T. Weyhermüller, E. Bill, K. Wieghardt, Inorg. Chem. 39 (2000) 930.
[3] A. Görling, Phys. Rev. A 47 (1993) 2783.
[4] Á. Nagy, Phys. Rev. A 57 (1998) 1672.
[5] G. te Velde, E.J. Baerends, J. Comput. Phys. 99 (1992) 84.
[6] Vrije Universiteit, De Boelelaan 1083, 1081 HV Amsterdam, The Netherlands, ADF documentation, June 1999.
[7] R. Parr, W. Yang, Density-Functional Theory of Atoms and Molecules, Oxford University Press, Oxford, 1989 Chapter 7.
[8] C.E. Schäffer, in: W.C. Price, S.S. Chissick, T. Ravensdale (Eds.), Wave Mechanics—the First Fifty Years, Butterworths, London, 1973.
[9] H. Bethe, Ann. Physik 3 (1929) 133.
[10] J.H. van Vleck, J. Chem. Phys. 3 (1935) 803.
[11] J.H. van Vleck, J. Chem. Phys. 3 (1935) 807.
[12] F.E. Ilse, Dissertation, Frankfurt a. M., 1946.
[13] F.E. Ilse, H. Hartmann, Z. Naturforschg. 6a (1951) 751.
[14] L.E. Orgel, J. Chem. Soc. (1952) 4756.
[15] C.J. Ballhausen, Mat. Fys. Medd. Dan. Vid. Selsk. (1954) 29.
[16] C.K. Jørgensen, Acta Chem. Scand. 8 (1954) 1502.
[17] L.E. Orgel, J. Chem. Soc. (1955) 1004.
[18] L.E. Orgel, J. Chem. Soc. (1955) 1819.
[19] L.E. Orgel, J. Chem. Soc. (1955) 1824.
[20] C.E. Schäffer, C.K. Jørgensen, Mol. Phys. 9 (1965) 401.

[21] C.K. Jørgensen, Absorption Spectra and Chemical Bonding, Pergamon Press, Oxford, 1962.
[22] J. Ferguson, D.L. Wood, Aust. J. Chem. 23 (1970) 861.
[23] R.G. Woolley, Internat. Rev. Phys. Chem. 6 (1987) 93.
[24] M. Gerloch, R.G. Woolley, Prog. Inorg. Chem. 31 (1984) 371.
[25] C.E. Schäffer, Structure and Bonding (1973) 69.
[26] R.G. Woolley, Chem. Phys. Lett. 118 (1985) 207.
[27] C.E. Schäffer, Inorg. Chim. Acta 240 (1995) 581.
[28] E.V. Condon, G.H. Shortley, The Theory of Atomic Spectra, Cambridge University Press, Cambridge, 1935.
[29] M. Brorson, C.E. Schäffer, Inorg. Chem. 27 (1988) 2522.
[30] M. Brorson, G.S. Jensen, C.E. Schäffer, J. Chem. Educ. 63 (1986) 387.
[31] J. Bendix, M. Brorson, C.E. Schäffer, Coord. Chem. Rev. 94 (1989) 181.
[32] J. Bendix, M. Brorson, C.E. Schäffer, Oxidation states and d^q configurations in inorganic chemistry, in: G.B. Kauffman (Ed.), ACS Symposium Series, vol. 565, American Chemical Society, 1994, p. 213.
[33] C.K. Jørgensen, Prog. Inorg. Chem. 4 (1962) 73.
[34] C.K. Jørgensen, Modern Aspects of Ligand Field Theory, North-Holland Publishing Company, Amsterdam, London, 1971.
[35] C.K. Jørgensen, Oxidation Numbers and Oxidation States, Springer-Verlag, Berlin, 1969.
[36] C.E. Schäffer, Inorg. Chim. Acta 300 (2000) 1053.
[37] C.E. Schäffer, C.K. Jørgensen, J. Inorg. Nucl. Chem. 8 (1958) 143.
[38] C.E. Schäffer, J. Inorg. Nucl. Chem. 8 (1958) 149.
[39] J.S. Griffith, The Theory of Transition-Metal Ions, Cambridge University Press, Cambridge, 1961.
[40] R. Åkeson, L.G.M. Petterssson, M. Sandström, U. Wahlgren, J. Am. Chem. Soc. 116 (1994) 8691.
[41] J. Landry-Hum, G. Bussiére, C. Daniel, C. Reber, Inorg. Chem. 40 (2001) 2595.
[42] M. Brorson, T. Damhus, C.E. Schäffer, Comments Inorg. Chem. 3 (1983) 1.
[43] Y. Tanabe, S. Sugano, J. Phys. Soc. Japan 9 (1954) 753.
[44] C.K. Jørgensen, Quimica Nova 11 (1988) 10.
[45] J. Bendix, M. Brorson, C.E. Schäffer, Inorg. Chem. 32 (1993) 2838.
[46] C.E. Schäffer, Physica 114A (1982) 28.
[47] S.E. Harnung, C.E. Schäffer, Structure and Bonding 12 (1972) 201.
[48] S.E. Harnung, C.E. Schäffer, Structure and Bonding 12 (1972) 257.
[49] T. Ziegler, A. Rauk, E.J. Baerends, Theoret. Chim. Acta 43 (1977) 261.
[50] E. Baerends, V. Brandchadell, M. Sodupe, Chem. Phys. Lett. 265 (1997) 481.
[51] R. Stowasser, R. Hoffmann, J. Am. Chem. Soc. 121 (1999) 3414.
[52] J.P. Perdew, J.A. Chevary, S.H. Vosko, K.A. Jackson, M.R. Pederson, D.J. Singh, C. Fiolhais, Phys. Rev. B 46 (1992) 6671.
[53] M.R. Bray, R.J. Deeth, V.J. Paget, P.D. Sheen, Int. J. Quant. Chem. 61 (1996) 85–91.
[54] C.K. Jørgensen, Solid State Phys. 13 (1962) 375.
[55] C. Daul, Int. J. Quant. Chem. 52 (1994) 867.
[56] J. Katriel, R. Pauncz, Adv. Quant. Chem. 10 (1977) 143.
[57] J. Li, L. Noodleman, D.A. Case, in: E.I. Soloman, A.B.P. Lever (Eds.), Inorganic Electronic Structure and Spectroscopy, vol. 1, John Wiley, New York, 1999 Chapter 11.
[58] L. Noodleman, J. Chem. Phys. 74 (1981) 5737.
[59] J.C. Slater, Phys. Rev. 165 (1968) 655.